1991

Alleviation of interferences and reduction of sample memory in inductively coupled plasma mass spectrometry

Fred Grover Smith
Iowa State University

Order Number 9202389

Alleviation of interferences and reduction of sample memory in inductively coupled plasma mass spectrometry

Smith, Fred Grover, Ph.D.

Iowa State University, 1991

U·M·I
300 N. Zeeb Rd.
Ann Arbor, MI 48106

Alleviation of interferences and reduction of sample memory in inductively coupled plasma mass spectrometry

by

Fred Grover Smith

A Dissertation Submitted to the
Graduate Faculty in Partial Fulfillment of the
Requirements for the Degree of
DOCTOR OF PHILOSOPHY

Department: Chemistry
Major: Analytical Chemistry

Approved:

Signature was redacted for privacy.

In Charge of Major Work

Signature was redacted for privacy.

For the Major Department

Signature was redacted for privacy.

For the Graduate College

Iowa State University
Ames, Iowa
1991

TABLE OF CONTENTS

GENERAL INTRODUCTION

Since 1980, inductively coupled plasma mass spectrometry (ICP-MS) has emerged as an important technique for trace elemental analysis. The origins of the technique can be traced to the development of the ICP as an excitation source for atomic emission spectroscopy (AES) by Fassel in the late 1960s (1-3). In 1975, Gray demonstrated that mass spectra could be obtained from solutions introduced into a dc plasma (4,5), and the first analytical mass spectra of the ICP were reported by Houk in 1978 (6). Commercial application of ICP-MS followed when SCIEX, Inc. from Canada introduced its instrument at the 1983 Pittsburgh Conference. Since that time ICP-MS has experienced rapid growth as evidenced by five present manufacturers (SCIEX, Inc., VG Isotopes, Seiko, Yokogawa, and Turner Scientific) and the installation of approximately 600 instruments worldwide. Indeed, ICP-MS has been recognized as one of the "hottest" areas in science (7). A brief outline of the working principles of ICP-MS follows; further details are available in a number of recent reviews (8-11).

The ICP is an excellent ion source, with 54 elements ionized with an efficiency of greater than 90% (8). However, the ICP, usually sustained in argon, operates at atmospheric pressure. A mass spectrometer requires high vacuum ($< 10^{-5}$ torr), so the "trick" that makes the technique work involves overcoming this large pressure differential. The solution is the use of a differentially pumped interface to reduce the pressure in stages.

In most ICP-MS devices, the ICP torch is mounted horizontally, and the plasma is immersed into a metal cone on the interface called the sampler (Figure 1). The sampler is water-cooled and has a sampling orifice (~ 1 mm diam.) drilled in its tip. Gas from the central channel of the ICP flows through the orifice into the first stage of the vacuum chamber. A mechanical pump maintains a pressure of ~ 1 torr in this stage. As the gas enters this region of reduced pressure, a supersonic jet forms downstream from the sampling orifice. The center of the jet flows through a second orifice (~ 1 mm diam.) in another metal cone called the skimmer. Ions from the jet then enter the high vacuum region (~ 10^{-5} torr) of the mass spectrometer. A series of ion lenses (metal cylinders and plates) biased at appropriate voltages serve to focus and transmit the ions to the mass spectrometer.

For ICP-MS a quadrupole usually serves as the mass analyzer. A quadrupole consists of an array of four metal rods biased at rf and dc voltages. Only ions of a selected mass to charge ratio (m/z) have a stable path through the array; the others will strike the rods and be lost (12). The selected ions are then focused onto a detector, usually a Channeltron electron multiplier. This device is operated in a pulse-counting mode so discrete pulses from individual ions can be measured (13).

The detection limits obtainable by commercial ICP-MS devices range from 0.005 $\mu g\ L^{-1}$ to 0.05 $\mu g\ L^{-1}$ for over 60 elements; they are particularly good for heavy elements such as the rare earths.

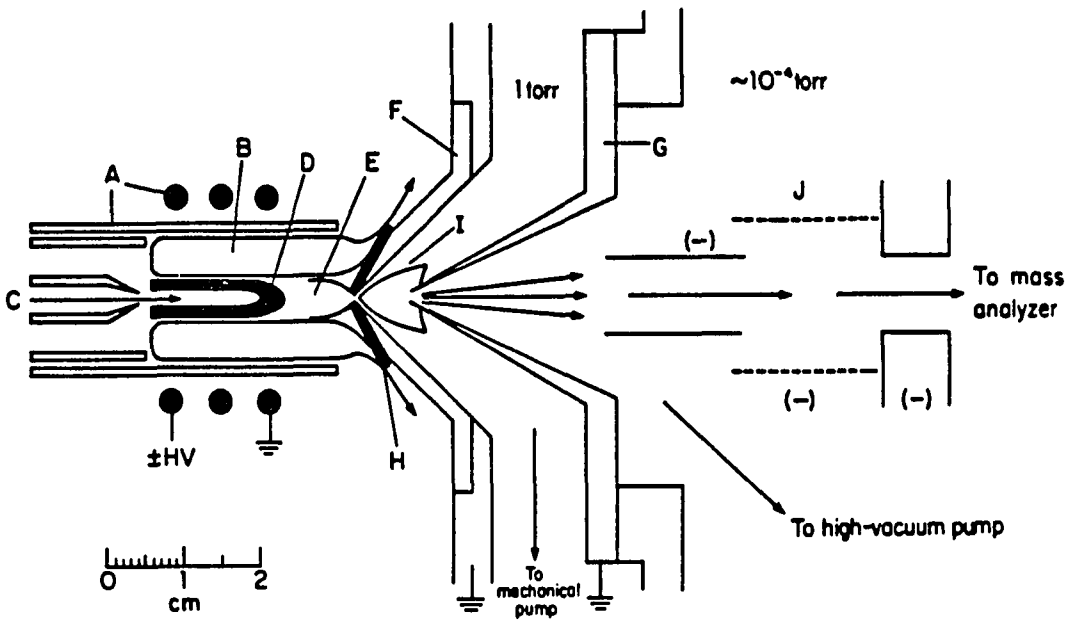

Figure 1. ICP and sampling interface. (A) torch and load coil (HV = high voltage), (B) induction region of ICP, (C) solution aerosol being injected into axial channel, (D) initial radiation zone, (E) normal analytical zone, (F) sampler cone with orifice in the tip, (G) skimmer cone, (H) boundary layer of ICP gas deflected outside sampling orifice, (I) expanding jet of gas sampled from ICP, and (J) ion lens elements. Reproduced from reference (8) with permission

Currently, ICP-MS exhibits the lowest detection limits of any multielement technique. In addition, isotope ratios can be determined with precisions of 0.2% to 1% relative standard deviation (RSD), allowing the use of stable isotopes in tracer studies and isotope dilution for elemental determinations. Thermal ionization mass spectrometry (TIMS) has traditionally been used for these applications because of the high precision (0.001% to 0.01%) obtained for isotope ratios. Such precision permits use of small amounts of often very expensive enriched stable isotopes since a slight change in the natural abundance ratio can be measured. However, sample preparation is complicated and sample throughput slow. ICP-MS can analyze ten or more samples per hour because samples are introduced as solutions at atmospheric pressure. Finally, the mass spectra in ICP-MS are inherently very simple at higher mass ($m/z > 80$), with minimal overlap interferences from other species. In contrast, atomic emission spectra from ICP-AES are complicated from features due to complex energy level structures of heavier elements. Weak emission lines and the greater possibility of spectral overlap interferences hamper the determination of these elements.

With these advantages there has been explosive growth in the applications of ICP-MS. Recent applications include trace elemental analysis of geological (14-27), environmental (28-39) and biological and clinical samples (40-66). Furthermore, ICP-MS has been used as an element-selective detector for chromatography (42-44, 67-71).

Since most samples are in solution form, nebulization is necessary for sample introduction to the ICP. Pneumatic nebulizers (72-76) are most commonly used for ICP-MS, but ultrasonic nebulizers (77-81) have also been used as they offer approximately a ten fold increase in sensitivity. Nonetheless, determination of a number of elements below m/z = 80 is difficult or impossible because of spectral interferences arising from argon, injected water, the sample matrix, or mineral acids used for sample preparation. These interferences have been extensively tabulated (82,83). Sample "memory effects", requiring lengthy cleanout times (> 5 min) between samples, are a major obstacle for determination of volatile elements such as I and Hg because of large dead volumes from spray chambers and sample introduction lines for these nebulizers. Finally, the low sample transport efficiency of a pneumatic nebulizer (~ 1%) or an ultrasonic nebulizer (~ 10%) means most of the sample is wasted. At least 5 to 10 mL of sample are required for an accurate analysis, and this volume may not be available in all applications, most notably biological and clinical samples.

Explanation of dissertation format

The focus of this dissertation is the alleviation of some spectral interferences below m/z = 80 and the reduction of sample memory. The alternate format is used for this dissertation. Each section stands independent of the others as a complete scientific manuscript with accompanying tables, figures, and literature cited. References cited

in this general introduction and the summary are given after the summary.

In the first section, a method for the determination of chlorine isotope ratios is described. Samples are dissolved in D_2O instead of water; $^{36}ArD^+$ at m/z = 38 is formed rather than the usual $^{36}ArH^+$, which interferes with $^{37}Cl^+$.

In the second section, boron concentrations are determined for a variety of biological samples by isotope dilution. A sample preparation method is described which avoids boron contamination and loss. Samples are introduced to the ICP-MS with a direct injection nebulizer (DIN) (84) which provides a much more rapid cleanout and a lower background than a concentric pneumatic nebulizer.

Analytical figures of merit for an Ar-Xe plasma are described in the third section. Introduction of xenon gas to the central channel of the ICP attenuates N_2^+, ArH^+, ClO^+, ArN^+, ArO^+ and other polyatomic ions by two to three orders of magnitude. Ion signals can be measured for Si, K, V, Cr, and Fe with little or no background correction, enabling accurate measurement of isotope ratios.

In the last section, fundamental measurements of the Ar-Xe plasma are described. No significant change occurs to the electron density (n_e) or the excitation temperature (T_{exc}) when xenon is added. However, a decrease in the ionization temperature (T_{ion}) is observed. The same measurements are described for addition of krypton, another noble gas used for comparison purposes. In this case addition of krypton did not appreciably affect the above parameters. Furthermore,

krypton reduced the polyatomic ions listed above by only factors of 1 to 4. Also, a Cs matrix study was performed in an attempt to mimic the effect of added xenon on analyte signal. Results indicate that the main source of ion loss upon addition of xenon is primarily a matrix effect, but the drop in T_{ion} may explain the preferential loss of interfering polyatomic ions versus analyte ions.

SECTION I.

ALLEVIATION OF POLYATOMIC ION INTERFERENCES FOR DETERMINATION OF CHLORINE ISOTOPE RATIOS BY INDUCTIVELY COUPLED PLASMA MASS SPECTROMETRY

INTRODUCTION

Inductively coupled plasma mass spectrometry (ICP-MS) is a fast method for the determination of elemental concentrations and stable isotope ratios in solutions (1-6). Determination of isotope ratios for the intracellular electrolytes magnesium, potassium, and chlorine is important for monitoring physiological function (7-10). The determination of Mg is straightforward (11), but K requires major modification of plasma operating conditions (12) or use of a completely different plasma (13) or flame (14). Determination of Cl is difficult for two reasons. First, the degree of ionization of Cl is only ~ 0.1 - 1% in the plasma (15), so the sensitivity is lower than for other elements. Second, the major polyatomic ion $^{36}ArH^+$ overlaps with $^{37}Cl^+$. Chlorine can be detected as the negative ion Cl^- by ICP-MS, but the high background degrades detection limits (16,17). A helium-supported ICP has been studied with ICP-MS for the detection of chlorine in gaseous organic samples (18). However, the introduction of water often destabilizes helium plasmas and causes poor or erratic performance. Recently, a helium microwave-induced plasma (MIP) coupled to a mass spectrometer has demonstrated a Cl detection limit of 39 $\mu g\ L^{-1}$ for aqueous samples, but an isotope ratio was not reported (19). Bromine is more readily measured and has been proposed as a substitute for Cl in physiological experiments (20), but a direct determination of Cl is also desirable.

This paper describes a simple procedure which allows the measurement of Cl isotope ratios using Cl^+. The sample is dissolved in 99.9% D_2O, so little nebulized water is injected into the plasma. Because most of the hydrogen comes from the injected water, the problematic polyatomic ion is now $^{36}ArD^+$ at m/z = 38. The $^{36}ArH^+$ background decreases, which facilitates determination of ^{37}Cl.

EXPERIMENTAL

Instrumentation

The ELAN Model 250 with upgraded ion optics (Perkin-Elmer SCIEX, Thornhill, Ontario, Canada) was used. The cryopump and mass spectrometer electronics were cooled with an HX-150 recirculating water chiller (Neslab Instruments, Portsmouth, NH). The water temperature was set at 10 ^{o}C. The nebulizer gas flow rate was regulated by a mass flow controller (Model 8200, Matheson Scientific, East Rutherford, NJ). Samples were introduced to the nebulizer at a rate of 0.5 mL min^{-1} by a Rainin minipuls 2 peristaltic pump (Rainin Instrument Co., Woburn, MA). The continuous flow ultrasonic nebulizer was operated at a forward power of 40-45 W (21,22). The wet aerosol was desolvated with a heating chamber (200 ^{o}C) and a condenser (0 ^{o}C) (22) and was transported to the plasma through Tygon tubing (~ 1 m long).

Chemicals and sample preparation

The 99.9% D_2O was obtained from Cambridge Isotope Laboratories (Woburn, MA). Lithium chloride from Fisher Scientific (Fair Lawn, NJ) was used as the source of chlorine. This compound was chosen because the light Li^+ ion should cause less suppression of Cl^+ signal than a heavier counter ion like K^+ or Na^+ (23,24). High purity deionized water (resistance ~ 18 MΩ) was obtained from a Barnstead Nanopure-II

system (Barnstead Co., Newton, MA). A 50 mg L^{-1} Cl solution was prepared in D_2O. The LiCl used was dried in an oven at 250 ^{o}C and stored in a desiccator. An accurately weighed amount of LiCl was then dissolved directly in 50.0 mL of D_2O.

Instrumental conditions

General instrumental and sampling conditions are given in Table I. Isotope ratios were measured in a peak hopping mode, and spectra were obtained by scanning, as described in Table I. Before each experiment, the sample introduction system was kept as free from water as possible in the following ways. The spray chamber of the nebulizer and the desolvation system were dried with a heat gun. In addition, the waste U-tube leading from the spray chamber and the condenser was filled with D_2O. Operating conditions for the instrument were adjusted to maximize the signal from $^{36}Ar^{+}$ while nebulizing D_2O. This procedure was employed because nebulization of aqueous standard solutions during optimization of operating conditions would have contaminated the sample introduction device with water.

RESULTS AND DISCUSSION

Mass spectra

The background mass spectrum obtained during nebulization of D_2O is shown in Figure 1. The major background ions in the given mass range are $^{16}O_2^+$, $^{36}Ar^+$ and both $^{38}Ar^+$ and $^{36}ArD^+$ at m/z = 38. The injection of D_2O yields a peak at m/z = 34 which is from DO_2^+.

The magnitude of the background at m/z = 35 and 37 is shown in Table II. Most of the background at m/z = 37 is probably from residual $^{36}ArH^+$. Hydrogen, water, or hydrocarbons in the argon and water impurity in the D_2O are the likely sources of hydrogen. Numerous polyatomic ions contribute to the background at m/z = 35; these are probably $^{16}O^{17}OD^+$, $^{17}O^{17}OH^+$, $^{18}O^{16}OH^+$, and $^{17}O^{18}O^+$.

A spectrum obtained during nebulization of the LiCl sample (50 mg L^{-1} in D_2O) is shown in Figure 2. Both chlorine isotopes (m/z = 35 and 37) were clearly observed. The background peaks at m/z = 36 and 38 are suppressed by approximately 40% relative to the count rates seen from the D_2O blank solution. The DO_2^+ peak at m/z = 34 is about the same intensity in Figures 1 and 2.

Deionized water was then introduced into the ICP. The count rate at m/z = 37 was monitored in the multielement mode until a steady value was reached. The nebulizer and desolvation system became saturated with water in approximately 30 min. The background mass spectrum from deionized water was then obtained (Figure 3). A

substantial peak from $^{36}ArH^+$ is readily apparent at m/z = 37. In addition, the DO_2^+ peak at m/z = 34 has been replaced by HO_2^+ at m/z = 33. The count rates given in Table II show that injection of D_2O rather than H_2O reduces the background at m/z = 37 by almost a factor of ten. The background at m/z = 35 is still modest when D_2O is nebulized; an increase of a factor of two is indicated. Thus, m/z = 35 remains fairly clear.

Isotope ratio measurements

Isotope ratio and sensitivity data for the 50 mg L^{-1} solution of Cl in D_2O are shown in Table III. These data were obtained using a very short dwell time (1 ms) so more measurements could be taken in the 1.0 s measurement time. Rapid measurements may help average out fluctuations in the intensity of the ion beam (26,27). However, the acquisition of twenty ratio measurements takes approximately 12 minutes due partly to a 4-ms computer overhead between hops. Nonetheless, if samples containing Cl are sufficiently concentrated (10-100 mg L^{-1}), then the Cl^+ signal is high enough for the remaining background to be unimportant.

In this case, the precision for the ratio $^{35}Cl/^{37}Cl$ was 0.21% RSD, which was comparable to that expected from counting statistics based on the total counts accumulated for each peak. Similar precision was obtained when the experiment was repeated on a different day. The close agreement between the experimental precision and that expected from counting statistics is unusual. For ion count rates in the range

10^5 to 10^6 counts s^{-1}, the experimental precision for isotope ratios measured with this particular instrument (and others like it) is generally worse than the precision expected from counting statistics by a factor of two to four (5,6,10,12,27,28,30). The fast peak hopping (dwell time 1 ms) employed in the present work may help improve precision, as indicated in other, preliminary measurements with silver and zinc (27). The RSD in the isotope ratio (0.21%) was much better than the RSD of 1.8% for the count rates for either $^{35}Cl^+$ or $^{37}Cl^+$. These latter RSDs are typical of the short-term precision in the signal achievable by present ICP-MS devices at these count rates. They are well above the counting statistical values of 0.1% to 0.2% (not shown in Table III).

The determined value for the $^{35}Cl/^{37}Cl$ ratio in Table III is about 9% below the accepted natural abundance ratio. Mass bias effects for other isotopes 2 m/z units apart can cause determined ratios to deviate from accepted values by 2-10% (2,4,30,31). The somewhat low value for the ratio $^{35}Cl^+/^{37}Cl^+$ may also have been caused by loss of gain in the detector during measurement of $^{35}Cl^+$, which was quite possible at count rates approaching 10^6 counts s^{-1} (32,33). Plasma operating conditions and ion lens voltages are known to influence isotope ratio values (12), but no experiments with these parameters were performed due to the limited amount of D_2O available.

The detection limit (i.e., the solution concentration necessary to yield a net signal equivalent to three times the standard deviation of the background) was 20 $\mu g\ L^{-1}$ for chlorine using $^{35}Cl^+$. This value is

comparable to other detection limits reported for Cl as Cl^- from an Ar ICP (16,17) or Cl^+ from a He MIP (19). Typically, we observe ion count rates of ~ 10^6 counts s^{-1} per mg L^{-1} for a metal ion of medium mass (m/z ~ 23 to 60) that would be expected to be nearly 100% ionized in the ICP. Comparison of this value to the $^{35}Cl^+$ count rate in Table III shows that Cl is of the order of 1% ionized, as expected (15).

Sample cleanout

Figure 4 shows a cleanout curve for the 50 mg L^{-1} sample in D_2O. The original signal for $^{35}Cl^+$ (~ 800,000 counts s^{-1}) decays to approximately 4500 counts s^{-1} after ~ 2 min. This level corresponds to about 0.5% of the original signal and is only several hundred counts s^{-1} above the D_2O background at m/z = 35 in Table II. Elements such as osmium, boron, and mercury that have forms that are volatile at the temperature of the heating chamber (200 ^oC) can suffer from long memory or loss with the desolvation system employed (22), but apparently this was not a problem for Cl in the present work.

This rapid cleanout of $^{35}Cl^+$ is necessary due to the expense of D_2O, and two simple measures greatly reduce sample memory. A fresh length of Tygon tubing was installed between the desolvator and the plasma, and the nebulizer spray chamber was soaked in concentrated H_2SO_4 for 24 h. The former provided an aerosol conduit free from long-term sample memory, whereas the latter facilitated smooth drainage of condensed droplets from the walls of the spray chamber.

CONCLUSION

Sample dissolution in D_2O can significantly reduce the $^{36}ArH^+$ interference and allow the measurement of the $^{35}Cl/^{37}Cl$ ratio. The precision of 0.2% RSD is at least as good as that obtained in ICP-MS for other elements and approaches the 0.1% level desirable for widespread application studies (10). A substantial amount of chlorine (0.1 - 1 mg) is required, but most biological samples contain high concentrations of this element. For example, the normal chlorine content of human blood is ~ 100 mmol L^{-1} (34), from which a sample volume of only 30 μL is necessary to provide 0.1 mg of Cl. As in most present isotope tracer studies with ICP-MS, sample cleanup would likely be desirable to remove the biological matrix (proteins, etc.) and interfering metal ions such as Na^+ and K^+ (23,24). A blood sample could be centrifuged and the resulting serum transferred to a cation exchange column in the Li^+ form. The collected solution would be evaporated to dryness and reconstituted in D_2O. Such refinements in sample preparation should lead to a useful protocol for fast measurement of Cl isotope ratios by ICP-MS.

LITERATURE CITED

1. Dean, J. R.; Massey, R.; Ebdon, L. J. Anal. At. Spectrom. 1987, 2, 369.
2. Russ, G. P. III; Bazan, J. M. Spectrochim. Acta, Part B 1987, 42B, 49.
3. Longerich, H. P.; Fryer, B. J.; Strong, D. F. Spectrochim. Acta, Part B 1987, 42B, 39.
4. Ting, B. T. G.; Janghorbani, M. Spectrochim. Acta, Part B 1987, 42B, 21.
5. Serfass, R. E.; Thompson, J. J.; Houk, R. S. Anal. Chim. Acta 1986, 188, 73.
6. Janghorbani, M.; Ting, B. T. G.; Fomon, S. J. Am. J. Hematol. 1986, 21, 277.
7. Altura, B. M.; Durlach, J.; Seelig, M. S. Magnesium in Cellular Processes and Medicine; Karger: New York, 1987.
8. Whang, B. Potassium: Its Biological Significance; CRC Press: Cleveland, 1983.
9. Moore, F. D.; Oleson, K. H.; McMurrey, J. D.; Parker, H. V.; Ball, M. R.; Boyden, C. M. The Body Cell Mass and Its Supporting Environment; W. B. Saunders Company: Philadelphia, 1963.
10. Janghorbani, M., Department of Medicine, The University of Chicago, personal communication, 1989.
11. Schuette, S.; Vereault, D.; Ting, B. T. G.; Janghorbani, M. Analyst 1988, 113, 1837.

12. Jiang, S.-J.; Houk, R. S.; Stevens, M. A. Anal. Chem. 1988, 60, 1217.

13. Caruso, J. A.; Creed, J. T.; Shen, W. L. Presented at the 16th Annual FACSS Meeting, Chicago, IL, October 1989; paper no. 348.

14. Taylor, H. E.; Garbarino, J. R. Presented at the 30th Annual Rocky Mountain Conference, Denver, CO, August 1988; paper no. 175.

15. Houk, R. S. Anal. Chem. 1986, 97A, 58.

16. Fulford, J. E.; Quan, E. S. K. Appl. Spectrosc. 1988, 42, 425.

17. Vickers, G. H.; Wilson, D. A.; Hieftje, G. M. Anal. Chem. 1988, 60, 1808.

18. Montaser, A.; Chan, S.-K.; Koppenaal, D. Anal. Chem. 1987, 59, 1240.

19. Creed, J. T.; Davidson, T. M.; Shen, W. L.; Brown, P. G.; Caruso, J. A. Spectrochim. Acta, Part B 1989, 44B, 909.

20. Janghorbani, M.; Davis, T. A.; Ting, B. T. G. Analyst 1988, 113, 405.

21. Olson, K. W.; Haas, W. J., Jr.; Fassel, V. A. Anal. Chem. 1977, 49, 632.

22. Bear, B. R.; Fassel, V. A. Spectrochim. Acta, Part B 1986, 41B, 1089.

23. Tan, S. H.; Horlick, G. J. Anal. At. Spectrom. 1987, 2, 283.

24. Gillson, G. R.; Douglas, D. J.; Fulford, J. E.; Halligan, K. W.; Tanner, S. D. Anal. Chem. 1988, 60, 1472.

25. Scott, R. H.; Fassel, V. A.; Kniseley, R. N.; Nixon, D. E. Anal. Chem. 1974, 46, 75.

26. Douglas, D. J. Can. J. Spectrosc. 1989, 34, 38.

27. Houk, R. S.; Smith, F. G.; Wiederin, D. R.; Niu, H. Presented at the 16th Annual FACSS Meeting, Chicago, IL, October 1989; paper no. 592.

28. Egan, C. B.; Smith, F. G.; Houk, R. S.; Serfass, R. E. Am. J. Clin. Nutrition 1991, 53, 547.

29. Weast, R. C. (Ed.) CRC Handbook of Chemistry and Physics; CRC Press: Boca Raton, 1985-86; p B-238.

30. Houk, R. S.; Thompson, J. J. Mass Spectrom. Rev. 1988, 7, 425.

31. Russ, G. P. III; Bazan, J. M.; Date, A. R. Anal. Chem. 1987, 59, 984.

32. Huang, L.-Q.; Jiang, S.-J.; Houk, R. S. Anal. Chem. 1987, 59, 2316.

33. Kurz, E. A. Am. Lab. March 1979, 11, 67.

34. Benninghoven, J. L. (Ed.) Saunders Dictionary and Encyclopedia of Laboratory Medicine and Technology; Saunders: Toronto, 1984; p 297.

Table I. Operating conditions

ICP torch	Ames Laboratory design (25)
	Outer tube extended 30 mm from inner tubes
Forward power	1.25 kW
Argon flow rates (L min^{-1}):	
outer gas	13
auxiliary gas	0.2
aerosol gas	1.59
Sampling position	17 mm from load coil, on center
Sampler	Nickel, 1.1 mm diam. orifice
Skimmer	Nickel, 0.9 mm diam. orifice
Ion lens settings:	
Bessel box barrel	+5.4 V
Bessel box plate	-11.0 V
Einzel 1 and 3	-19.8 V
Einzel 2	-130 V
Bessel box stop	-4.9 V
Electron multiplier	
voltage	-3200 V
Operating pressures:	
interface	1 torr
quadrupole chamber	3×10^{-5} torr

Table I. (continued)

Data acquisition	Low resolution setting Measurements per peak spaced 0.1 m/z units about peak top $^{35}Cl/^{37}Cl$ ratio and background measurements: multielement monitoring mode, three measurements per peak, dwell time 1 ms at each position with total measurement time of 1.0 s. Cleanout study: multielement monitoring mode, three measurements per peak, dwell time 20 ms with total measurement time of 0.5 s. Spectra: sequential monitoring mode, 10 measurements per peak with measurement time of 1.0 s.

Table II. Background count rates

Blank solution	m/z = 35 mean (counts s^{-1})[a]	m/z = 35 RSD (%)[b]	m/z = 37 mean (counts s^{-1})[a]	m/z = 37 RSD (%)[b]
D_2O	3,900	2.6	5,900	2.8
H_2O	2,100	2.3	57,300	3.4

[a]Measurement time was 1.0 s.

[b]Relative standard deviation of 20 measurements.

Table III. Chlorine isotope ratio measurements[a]

^{35}Cl count rate (counts s^{-1})		^{37}Cl count rate (counts s^{-1})		Det'd $^{35}Cl/^{37}Cl$		RSD (%) for $^{35}Cl/^{37}Cl$
mean	RSD (%)	mean	RSD (%)	mean	RSD (%)	count. stats
793,000	1.8	277,200	1.8	2.861	0.21	0.22

[a]Mean and RSD of 20 measurements are reported. Measurement time was 1.0 s. Count rates are corrected for D_2O background. Accepted natural ratio = 3.127 (29).

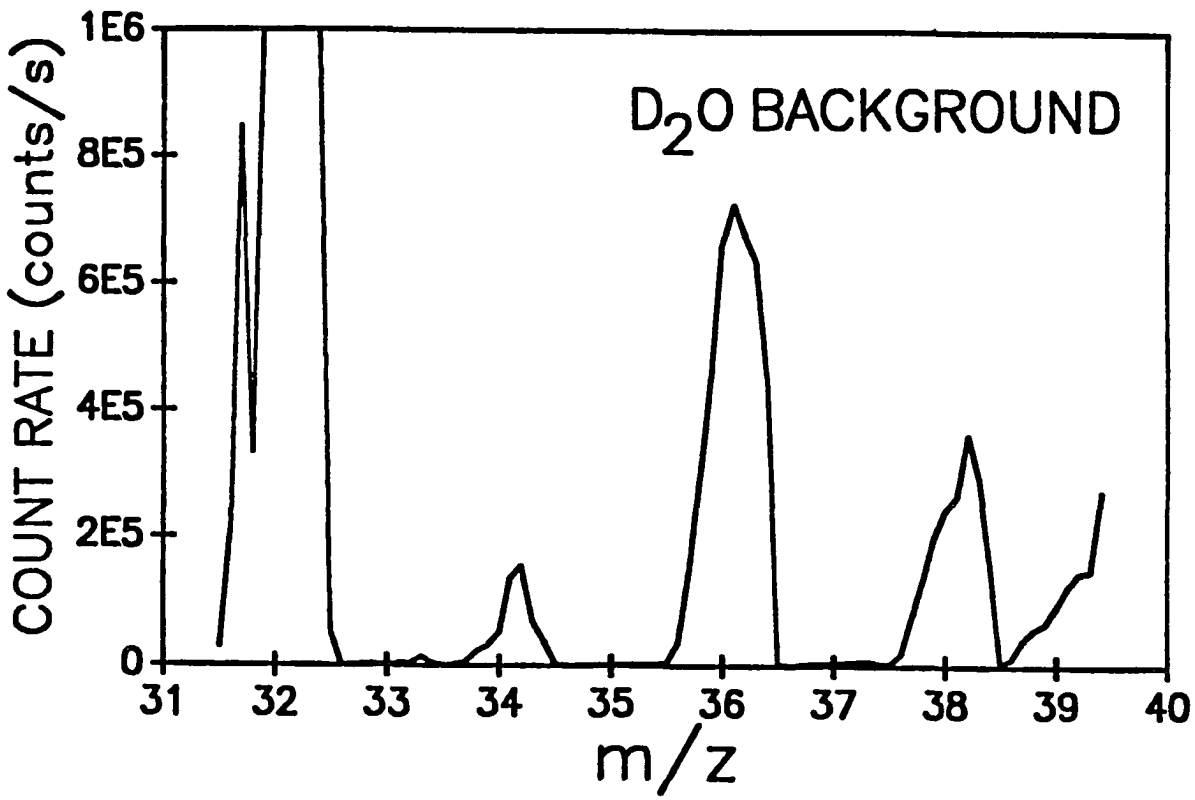

Figure 1. Background spectrum of 99.9% D_2O.

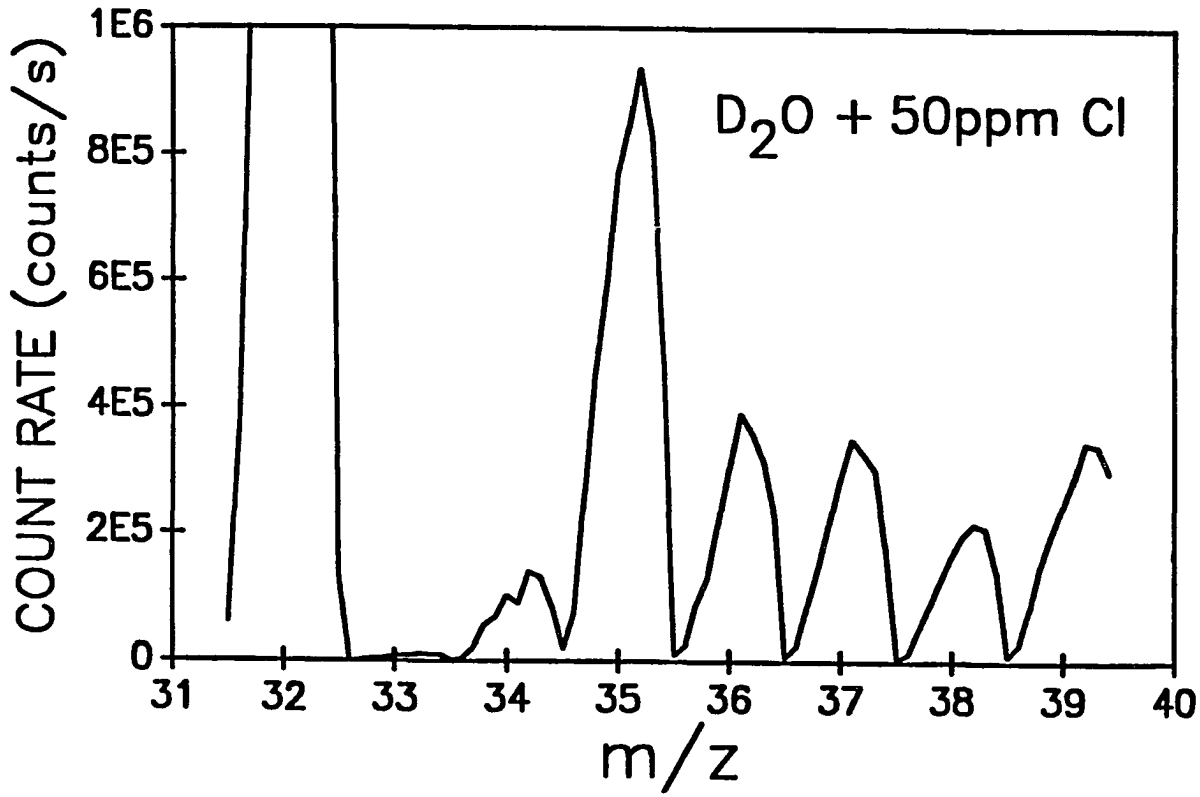

Figure 2. Spectrum of 50 mg L^{-1} Cl (as LiCl) in D_2O.

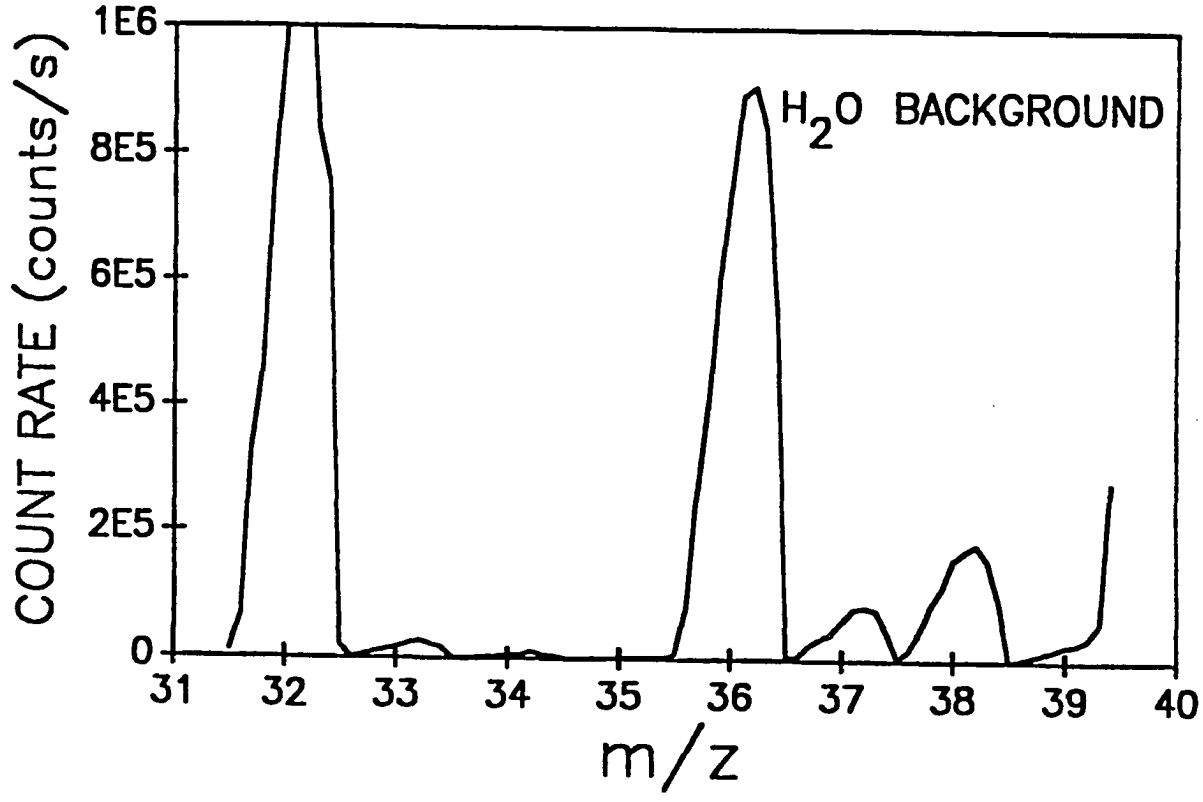

Figure 3. Spectrum of deionized H_2O.

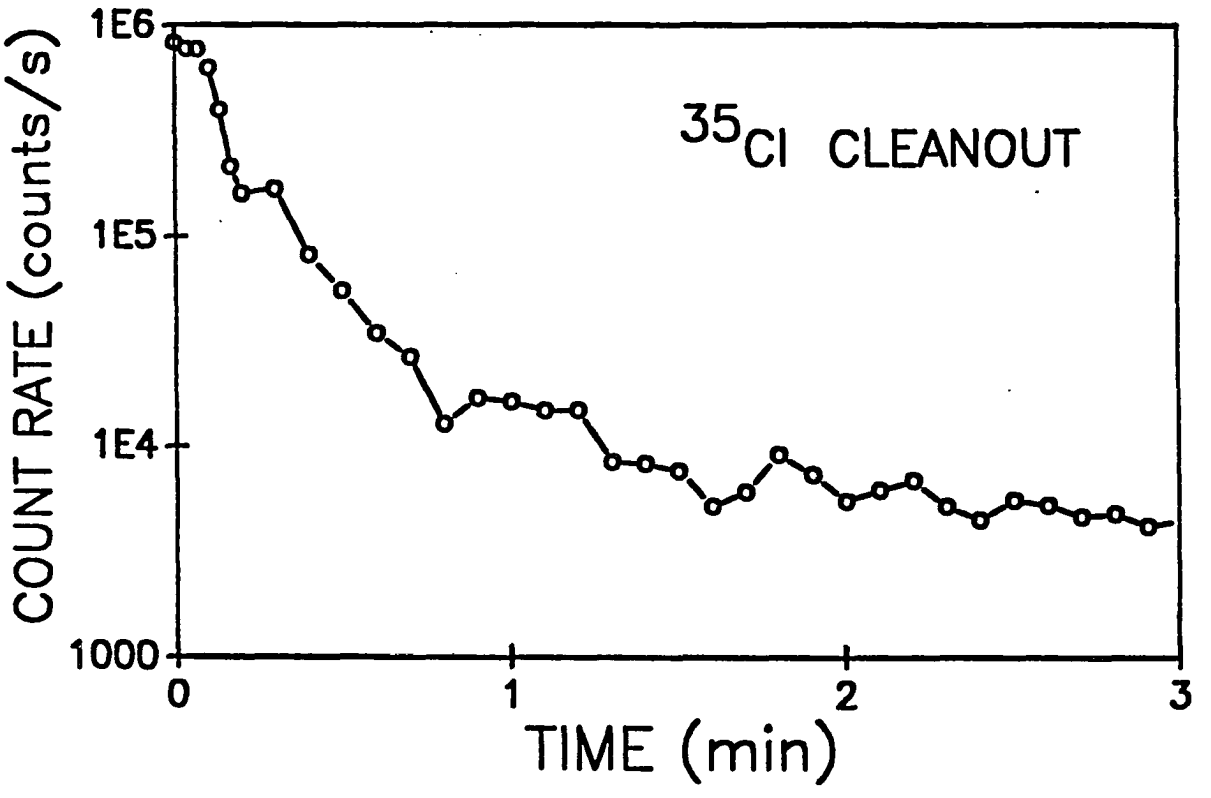

Figure 4. Cleanout curve for $^{35}Cl^{+}$.

SECTION II.

MEASUREMENT OF BORON CONCENTRATION AND ISOTOPE RATIOS IN BIOLOGICAL SAMPLES BY INDUCTIVELY COUPLED PLASMA MASS SPECTROMETRY WITH DIRECT INJECTION NEBULIZATION

INTRODUCTION

Boron is an essential element for higher plants, and recent evidence by Hunt and Nielsen supports its essentiality in animals (1,2). Furthermore, dietary boron markedly reduces urinary excretion of calcium and magnesium in postmenopausal women, suggesting a role for boron in prevention of osteoporosis (3).

To establish dietary requirements of boron in animals and humans, assessments of absorption, excretion, and tissue distribution of boron are needed. Accurate measurement of stable isotope ratios of boron and boron concentrations in biological samples are required because there are no radioisotopes of boron that are suitable as metabolic tracers and the natural abundance of stable isotopes of boron may differ from sample to sample.

Improved methodology for preparing biological samples for boron determination is necessary for several reasons. Boron concentrations in some animal tissues and fluids (e.g., blood serum) are so low as to be difficult to measure by existing methods. Samples can be readily contaminated with boron during wet ashing with mineral acids, particularly if borosilicate glassware is used. Hot mineral acids also may cause loss of volatile boron compounds (4). Another consideration is matrix-induced mass discrimination, which can be substantial because of the proportionally large mass difference between ^{10}B and ^{11}B. Gregoire shows that this type of interference

during ICP-MS measurements causes an increase in the measured ratio $^{11}B/^{10}B$ in the presence of an abundant matrix component like sodium (5). Finally, the intense peak from $^{12}C^+$ in biological samples can complicate measurement of $^{11}B^+$. Therefore, separation of boron from matrix components is advisable.

Methods for the determination of boron in biological samples include neutron-capture prompt γ-ray activation analysis (PGAA) (6,7), neutron-activation mass spectrometry (NA-MS) (8), thermal ionization mass spectrometry (TIMS) (9,10), inductively coupled plasma-atomic emission spectroscopy (ICP-AES) (11,12), and colorimetric (13) and potentiometric (14) methods. TIMS is capable of isotope ratio precisions between 0.2% and 0.3%. However, important disadvantages of some of the methods (PGAA, NA-MS, TIMS) include long sample preparation and analysis times and the limited availability of instruments. Furthermore, the only method applicable for samples that contain less than 300 ng of boron is NA-MS. ICP-MS has the advantage of faster analysis times, less complicated sample preparation, and high sensitivity (~ 1 ng g^{-1} detection limit) and selectivity. This method has been used for the determination of boron isotope ratios in geological samples that contained ~ 1 μg B with a precision of 0.7% (5). Recent work by Gregoire shows that boron in fresh and saline waters can be determined accurately by isotope dilution ICP-MS (15).

In the present work, conditions for separating boron from biological matrices for analysis by ICP-MS using direct injection nebulization (DIN) are reported. The DIN enables direct introduction

of aqueous samples into the ICP and permits analysis of small sample volumes (< 1 mL) at low concentrations of boron (< 30 $\mu g\ L^{-1}$). Most importantly, the DIN has a very low dead volume (~ 2 μL) and does not require a spray chamber. These features greatly reduce boron memory, which is a significant problem with conventional methodology for sample introduction. Samples are analyzed in only 3-4 minutes.

EXPERIMENTAL

Instrumentation

The ICP-MS used was the ELAN Model 250 with upgraded ion optics (Perkin-Elmer SCIEX, Thornhill, Ontario, Canada). The DIN has been described (16). The only modification was the substitution of Tefzel tubing for the Teflon-lined stainless steel tubing in the gas displacement pump. A Meinhard C3 concentric glass nebulizer with a Scott-type double pass spray chamber and a SCIEX long torch were used for the comparative boron cleanout study (i.e., for Figure 1 only). In this case a Rainin minipuls 2 peristaltic pump (Rainin Instrument Co., Woburn, MA) was used for solution uptake (2 mL min^{-1}). Instrument operating conditions with the DIN are listed in Table I.

Materials and reagents

National Institute of Standards and Technology (NIST) SRM 951 (isotopically analyzed boric acid) was used for instrument calibration. Enriched boric acid (94.56% ^{10}B) for calibration and isotope dilution was obtained from Eagle Picher (Quapaw, OK). Sodium carbonate was reagent grade from Fisher Scientific (Fair Lawn, NJ). Amberlite IRA-743 ion-exchange resin (20-50 mesh) from Rohm and Haas (Philadelphia, PA) was used to separate boron from samples and to remove residual boron from the sodium carbonate. Both nitric and hydrochloric acids were Ultrex II grade from J. T. Baker

(Phillipsburg, NJ). A 2% solution of this nitric acid was the carrier stream from the gas displacement pump. Ammonium hydroxide was isopiestically distilled (17) from Fisher reagent grade material, and deionized water (resistance ~ 18 MΩ) was obtained from a Barnstead Nanopure-II system (Newton, MA). Acid-washed (6M HCl) and fired (800 ^{o}C) 30-mL platinum crucibles were used for the fusions.

Preparation of columns and Na_2CO_3 solutions

Ion-exchange columns were prepared by adding approximately 1 mL of wet Amberlite IRA-743 resin to a 5-mL disposable polypropylene column from Isolab, Inc. (Akron, OH). The resin was contained between the polyethylene filter disks supplied with the columns. Before use each column was washed with 10 mL of water, 5 mL of 3 N NH_4OH, 20 mL of water, 10 mL of 1 M HCl, 5 mL of water, 10 mL of 1% HNO_3 and 20 mL of water. A 1 M Na_2CO_3 solution was prepared and 100-mL portions were cleaned of boron impurities by passage through one of the Amberlite columns. This cleaned Na_2CO_3 was used for all fusions.

Sample preparation

Four different types of samples were analyzed for boron content. Human blood plasma from healthy male volunteers was freshly separated by centrifugation from formed elements. Samples were pooled and stored in polyethylene at -20 ^{o}C. The other samples were reference materials from NIST: SRM 909 Human Serum, SRM 1571 Orchard Leaves and SRM 1548 Total Diet.

Each sample of pooled human plasma (10.0 mL each, pipetted with a Gilson Pipetman) was mixed with 10 mL of cleaned 1 M Na_2CO_3 and 0.20 μg of enriched ^{10}B in a separate platinum crucible. The mixture was frozen in the crucible and lyophilized for 24 h at 37 ^{o}C. Each crucible was then placed over a Bunsen burner and a small flow of oxygen was introduced from above while the dry, solid material within decomposed to ash (18). Residue was fused by use of a Meeker burner (~ 900 ^{o}C). Ashing and fusion took approximately 20 minutes. The fused residue in the crucible was dissolved in 3 mL of water, and 1.5 mL of 6 M HCl were added to lower the pH (~ 8). The resultant solution was added portionwise (~ 1.5 mL) to a separate column that was subsequently washed with seven 5-mL portions of water. Five 2-mL portions of 1% HNO_3 were used to elute boron from the column into a Falconware polystyrene tube (Becton-Dickinson, Linclon Park, NJ). Each blank consisted of a composite of all reagents except the sample; the same containers and procedures were used to prepare the blank.

Samples and blanks were then analyzed by ICP-MS. Solutions were loaded in a 0.5-mL Tefzel sample loop with disposable 1-mL polyethylene syringes (Becton-Dickinson) to avoid boron contamination.

The previous procedure also was used to prepare each biological reference material except for the following modifications. The Human Serum (SRM 909) was supplied as lyophilized material in sealed brown glass vials accompanied by diluent water in separate, sealed glass bottles. The diluent water was found to contain high concentrations of boron (~ 150 $\mu g\ L^{-1}$), so it was not used. The lyophilized material

from one vial was transferred directly to a platinum crucible and weighed accurately. The lyophilized material from a second vial was split into two crucibles and weighed accurately. The mass of the enriched ^{10}B spike was 0.20 μg. The Orchard Leaves (SRM 1571) were dried in a convection oven at 90 ^{o}C for 24 h, and accurately weighed samples (~ 0.3 g) were spiked with 10.0 μg of enriched ^{10}B. Total Diet (SRM 1548) was lyophilized as specified on the certificate in order to determine moisture content (found: 1.494%). As specified, the unlyophilized reference material (~ 0.5 g each time) was accurately weighed and spiked with 1.00 μg of enriched ^{10}B.

Isotope dilution analysis

Boron concentrations were calculated using the following equation:

$$C = \frac{M_S K(X_S - Y_S R)}{W(YR - X)}$$

where C is the boron concentration in micrograms per gram (or micrograms per milliliter), M_S is the mass of the enriched ^{10}B spike in micrograms, K is the ratio of the natural and spike atomic weights, X is the natural abundance of ^{10}B, Y is the natural abundance of ^{11}B, X_S is the abundance of ^{10}B in the spike, Y_S is the abundance of ^{11}B in the spike, W is the sample weight or volume, and R is the measured $^{10}B/^{11}B$ ratio. Standard boron references (SRM 951 and Eagle Picher enriched $H_3{}^{10}BO_3$) were used to calibrate the response of the mass spectrometer for ^{10}B relative to that for ^{11}B. The abundances

measured were used in all calculations to correct for mass bias in the instrument (19).

RESULTS AND DISCUSSION

Boron cleanout study

Figure 1 compares the cleanout characteristics of the DIN with those of a typical pneumatic nebulizer and spray chamber. Sensitivity (~ 9 x 10^5 counts s^{-1} ^{11}B) for a 1.6 mg L^{-1} B solution in 2% HNO_3 was similar for the two nebulizers even though the solution uptake rate for the DIN (100 μL min^{-1}) was 20x less than that for the Meinhard nebulizer. The rinse solution was 2% HNO_3 for both. The signal from the Meinhard nebulizer fell by an order of magnitude in approximately 30 s, but afterwards it decayed very slowly, reaching 2% of the original signal after a very long time interval (8 min). After switching out the sample loop, the signal from the DIN fell by three orders of magnitude in only 15 seconds. After 1 min the signal had fallen to approximately 300 counts s^{-1}, roughly 0.03% of the original signal. The sample loop required only a 3-mL rinse with 2% HNO_3, and the next sample could then be loaded. Furthermore, the lower background facilitates the measurement of low boron concentrations. The rapid cleanout of the DIN may also prove useful in boron determination by ICP-AES (20).

Boron recovery study

The boron recovery for the sample preparation procedure was investigated for Na_2CO_3 blanks and pooled human plasma. Two blanks

were spiked with 0.30 μg natural boron (SRM 951) and two were not. All four blanks were carried through the procedure. The solutions were then analyzed and the results were compared with those from a 30 μg L^{-1} B standard in 2% HNO_3 that had not been put through the procedure. The recovery was found to be 92%. Four plasma samples were treated as the blanks and recovery was 77%. One possible explanation for the lower recovery of boron from the plasma samples is the effect of matrix components in the plasma during the ion-exchange process. Recoveries of natural abundance boron standard solutions spiked with varying amounts of enriched ^{10}B showed that boron volatilization during sample decomposition with Na_2CO_3 was negligible and that recovery of boron standard from the resin was 80% to 95%.

Analysis of biological samples

Results for the analysis of pooled human blood plasma and SRM 909 Human Serum are given in Table II. The $^{10}B/^{11}B$ ratios for the blanks are near the natural abundance ratio (0.2469) (21), so there is still some boron contamination, probably from the Na_2CO_3. The precision of the isotope ratios in the spiked samples ranges from 1.0% to 1.5%. The precision values are consistent with those expected from counting statistics and should be adequate for boron isotope tracer studies. The boron concentrations in the pooled plasma are reproducible (± 1 μg L^{-1}), but some variation in the split SRM 909 sample (#2) is apparent (26 μg L^{-1} vs. 34 μg L^{-1}). Nonetheless, the determined boron concentrations for SRM 909 #1 and #2-2 agree. Since SRM 909 is not

certified for boron, this material might not be useful for interlaboratory comparisons. A recent study by NA-MS reports a boron value of 18 ± 1 $\mu g\ kg^{-1}$ in platelet-poor human plasma (22), which is in good agreement with all but one of the results in Table II. In the present study, the mass of boron was roughly 0.2 μg in a 10-mL aliquot of unspiked blood plasma that was eluted with 10 mL of 1% HNO_3. Inasmuch as less than 2 mL of eluent is needed to fill the 0.5 mL sample loop of the DIN, the analytical procedure for boron in blood plasma could be scaled down by a factor of at least five, requiring about 2 mL of plasma for satisfactory results.

Results for the analysis of SRM 1571 Orchard Leaves and SRM 1548 Total Diet are given in Table III. Again, the isotope ratios for the blanks indicate some boron contamination but the sample ratios are more precise (0.4% to 0.6% RSD) because the boron signal is much greater. The boron concentration in each sample is listed, with the results for SRM 1571 giving a mean value of 35.5 ± 2.2 $\mu g\ g^{-1}$ boron (95% confidence interval). This agrees well with the certified value of 33 ± 3 $\mu g\ g^{-1}$ boron. The mean value of the six SRM 1548 samples is 2.53 ± .05 $\mu g\ g^{-1}$ boron (95% confidence interval), which is in excellent agreement with a reference value of 2.5 $\mu g\ g^{-1}$ boron.

CONCLUSION

The use of a DIN for sample introduction for ICP-MS facilitates the rapid analysis of boron-containing solutions by drastic reduction of sample memory and sample consumption. Sample preparation is still necessary for removal of matrix components from biological samples, but use of isotope dilution allows accurate boron determinations. Applications of the technique will involve tracer studies in animals and/or humans, which will be challenging since boron concentrations are expected to be low. Further improvements in precision of isotope ratio measurements would be helpful for studies involving serum samples.

LITERATURE CITED

1. Hunt, C. D.; Nielsen, F. H. Trace Element Metabolism in Man and Animals; Howell, J. McC., Gawthorne, J. M., White, C. L., Eds.; Australian Academy of Science: Canberra, 1981; Vol. 4, pp 597-600.
2. Nielsen, F. H. Trace Elements in Environmental Health; Hemphill, D. D., Ed.; University of Missouri Press: Columbia, 1984; Vol. 18, pp 47-52.
3. Nielsen, F. H.; Hunt, C. D.; Mullen, L. M.; Hunt, J. R. FASEB J. 1987, 1, 394.
4. Nemodruk, A. A.; Karalova, Z. K. Analytical Chemistry of Boron; Kondor, R., Trans.; Israel Program for Scientific Translations: Jerusalem, 1965.
5. Gregoire, D. C. Anal. Chem. 1987, 59, 2479.
6. Falley, M. P.; Anderson, D. L.; Zoller, W. H.; Gordon, G. E.; Lindstrom, R. M. Anal. Chem. 1979, 52, 2209.
7. Anderson, D. L.; Cunningham, W. C.; Mackey, E. A. Fres. J. Anal. Chem. 1990, 338, 554.
8. Iyengar, G. V.; Clarke, W. B.; Downing, R. G. Fres. J. Anal. Chem. 1990, 338, 562.
9. Spivak, A. J.; Edmond, J. M. Anal. Chem. 1986, 58, 31.
10. Duchateau, N. L.; Verbruggen, A.; Hendrickx, F.; DeBievre, P. Anal. Chim. Acta 1987, 196, 41.

11. Mauras, Y.; Ang, K. S.; Simon, P.; Tessier, B.; Cartier, F.; Allain, P. Clin. Chim. Acta 1986, 156, 315.

12. Kumamaru, T.; Matsuo, H.; Okamoto, Y.; Yamamoto, M.; Yamamoto, Y. Anal. Chim. Acta 1986, 156, 315.

13. Weeth, H. J.; Speth, C. F.; Hanks, D. R. Am. J. Vet. Res. 1981, 42, 474.

14. Carlson, R. M.; Paul, J. L. Soil Sci. 1969, 108, 266.

15. Gregoire, D. C. J. Anal. At. Spectrom. 1990, 5, 623.

16. Wiederin, D. R.; Smith, F. G.; Houk, R. S. Anal. Chem. 1991, 63, 219.

17. Zief, M.; Mitchell, J. W. Contamination Control in Trace Elemental Analysis; Wiley: New York, 1976; pp 102-106.

18. D'Silva, A. P.; Sarananthan, T. R.; Chandola, L. C. Spectrochemical Determination of Boron in Graphite; Atomic Energy Establishment Trombay: Bombay, India, 1964; pp 1-8.

19. Dodson, M. H. J. Sci. Instrum. 1969, 2, 490.

20. Pougnet, M. A. B.; Orren, M. J. Intern. J. Environ. Anal. Chem. 1986, 24, 253.

21. Weast, R. C., Ed. CRC Handbook of Chemistry and Physics; CRC Press, Inc.: Boca Raton, 1985-86; p B-238.

22. Clarke, W. B.; Koekebakker, M.; Barr, R. D.; Downing, R. G.; Fleming, R. F. Appl. Radiat. Isot. 1987, 38, 735.

Table I. Operating conditions

ICP torch	Modified Sciex short torch: Injector tube orifice diam. = 1.75 mm 6 mm o.d. x 4 mm i.d. quartz tee attached at torch base.
Forward power	1.50 kW
Argon flow rates:	
outer	14 L min^{-1}
intermediate	1.4 L min^{-1}
DIN nebulizer gas (argon):	
pressure	100 psi
flow rate	0.5 L min^{-1}
additional make-up	0.25 L min^{-1}
Sampling position	20 mm from load coil, on center
Sample liquid flow rate	100 μL min^{-1}
Sampler	Copper, 1.1 mm diam. orifice
Skimmer	Nickel, 0.9 mm diam. orifice
Ion lens settings:	
Bessel box barrel	+5.4 V
Bessel box plate lens	-11.0 V
Einzel lenses 1 and 3	-19.8 V
Bessel box stop	-4.8 V

Table I. (continued)

Electron multiplier voltage	-4000 V
Operating pressures	
interface	1 torr
quadrupole chamber	3 x 10^{-5} torr
Flow injection valve	Rheodyne #9125 metal-free
	0.5 mL sample loop constructed from
	1/16" o.d. 0.5 mm i.d. Tefzel tubing
Data acquisition	Multielement Monitoring Mode (peak
	hopping)
	Low resolution, 1 measurement per
	peak
	Measurement time = 2.0 s
	Dwell time = 20 ms

Table II. Analytical results for pooled human blood plasma and SRM 909 Human Serum

Sample	Net ^{11}B count rate[a] (counts s^{-1})	Isotope ratio $^{10}B/^{11}B$	B concentration in original sample ($\mu g\ L^{-1}$)
blank[b]	925	0.2184[c]	--
Pooled #1	8,670	1.212 (1.3)	24 ± 4[d]
Pooled #2	8,100	1.211 (1.4)	24 ± 4
Pooled #3	6,770	1.265 (1.3)	22 ± 4
blank	740	0.2473	--
SRM 909 #1	9,760	2.548 (1.0)	26 ± 4
SRM 909 #2-1	6,690	2.143 (1.5)	34 ± 6
SRM 909 #2-2	5,350	2.477 (1.4)	26 ± 6

[a]Mean of 20 measurements.

[b]Mean of three blanks.

[c]Mean of 20 measurements, %RSD in parentheses.

[d]Uncertainty at 95% confidence interval.

Table III. Analytical results for SRM 1571 Orchard Leaves and SRM 1548 Total Diet

Sample	Net ^{11}B count rate[a] (counts s^{-1})	Isotope ratio $^{10}B/^{11}B$	B concentration in original sample ($\mu g\ g^{-1}$)
blank[b]	340	0.234[c]	----
SRM 1571 #1	405,000	1.311 (0.5)	34.5 ± .8[d]
SRM 1571 #2	414,700	1.310 (0.5)	34.9 ± .8
SRM 1571 #3	475,400	1.221 (0.4)	37.2 ± .6
blank	2,420	0.2169	----
SRM 1548 #1	205,400	1.106 (0.4)	2.59 ± .03
SRM 1548 #2	228,100	1.098 (0.4)	2.53 ± .03
SRM 1548 #3	236,500	1.126 (0.5)	2.49 ± .04
SRM 1548 #4	219,100	1.094 (0.4)	2.50 ± .03
SRM 1548 #5	225,100	1.145 (0.5)	2.49 ± .04
SRM 1548 #6	219,100	1.123 (0.6)	2.55 ± .04

[a]Mean of 20 measurements.

[b]Mean of three blanks.

[c]Mean of 20 measurements, %RSD in parentheses.

[d]Uncertainty at 95% confidence interval.

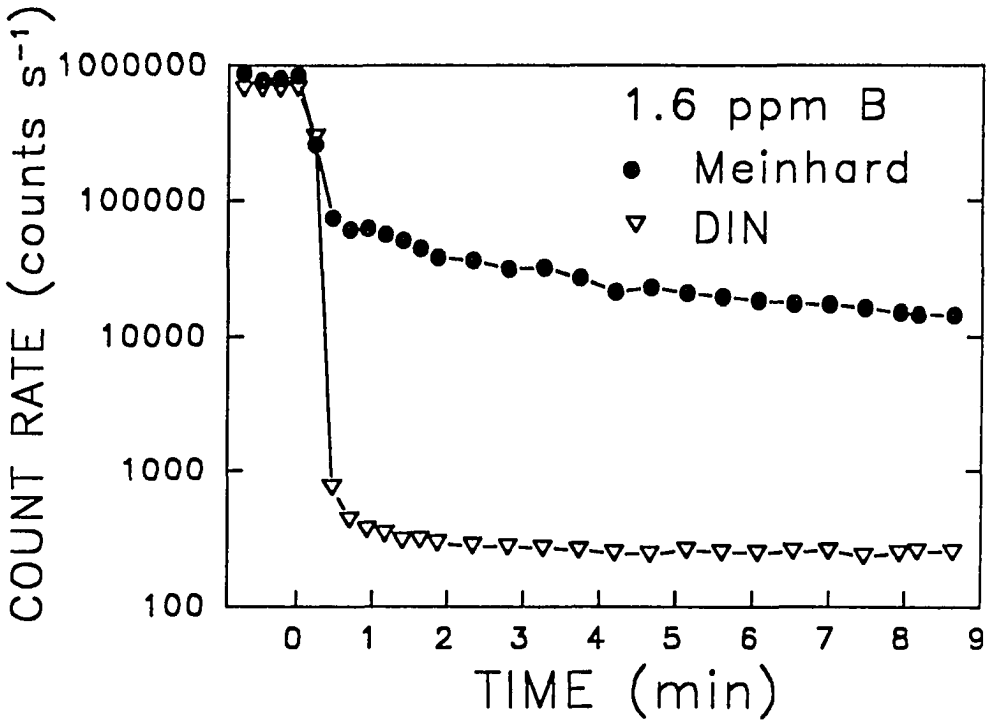

Figure 1. Comparative cleanout study of the DIN and a Meinhard C3 pneumatic nebulizer with a Scott-type double pass spray chamber. The sample was removed and cleanout began at time = 0 min

SECTION III.

AN ARGON-XENON PLASMA FOR ALLEVIATING POLYATOMIC ION INTERFERENCES IN INDUCTIVELY COUPLED PLASMA MASS SPECTROMETRY

INTRODUCTION

Inductively coupled plasma mass spectrometry (ICP-MS) is a sensitive, accurate, and precise method for trace multielemental and isotopic analysis of solutions (1-4). However, polyatomic ions arising from argon, water, and mineral acids cause substantial spectral overlap for a number of elements, especially below m/z = 80 (5,6).

Techniques for correction or attenuation of these ions are quite varied. The simplest approach is to subtract the background signal from the analyte peak, but this procedure becomes difficult for analyte signals just above the background. The count rates for background ions can also vary with the chemical identity and concentration of the sample matrix. Isotope ratios can be measured for either analyte or interferent to help correct for spectral overlap interferences (7), but unobstructed isotopes are not always available. Oxide and hydroxide ions derived from injected water can be reduced by desolvation (8,9) or, in some cases, by introducing the analyte as a hydride (10). Electrothermal vaporization (ETV) was used by Gray and co-workers to mitigate ArO^+ and $ArOH^+$ for the determination of iron isotope ratios (11). More drastic measures include use of a helium plasma (12,13) to attenuate ions containing argon or a high resolution mass spectrometer to resolve polyatomic ions and analyte ions of the same nominal mass (14).

Several other methods for attenuating polyatomic ions are related to the present work. Rowan and Houk added xenon to a quadrupole collision cell to remove ArO^+ (15). Evans and Ebdon introduced an organic solvent or a molecular gas into the central channel of the ICP to reduce $ArCl^+$ and Ar_2^+ for determination of arsenic and selenium (16). Lam and Horlick (17), Lam and McLaren (18), and Lam, McLaren and Gustavsson (19) added N_2 to the outer gas flow of an Ar ICP to attenuate a number of background ions (ArO^+, $ArOH^+$, Ar_2^+, ClO^+, and $ArCl^+$) by an order of magnitude. The general characteristics of mixed-gas ICPs are described in a recent review (20).

In the present work, small amounts of xenon (10 mL min^{-1} or 37 mL min^{-1}) are introduced into the central channel of the ICP. The count rates from various polyatomic ions are reduced more extensively than the count rates for analyte ions. The result is improved performance for measurement of several important elements (Si, K, V, Cr, and Fe), particularly for isotope ratio determinations.

EXPERIMENTAL

Instrumentation

The inductively coupled plasma mass spectrometer used was the ELAN Model 250 with upgraded ion optics (Perkin-Elmer SCIEX, Thornhill, Ontario, Canada). The argon in the aerosol gas flow was regulated by a mass flow controller (Model 8200, Matheson Scientific, East Rutherford, NJ). The continuous flow ultrasonic nebulizer was operated at a forward power of 40-45 W (21,22) and a solution uptake rate of 2.0 mL min^{-1}. The wet aerosol was desolvated with a heating chamber (200 ^{o}C) and a condenser (0 ^{o}C) (22). The resulting dry aerosol was transported to the plasma through 0.95 cm i.d. Tygon tubing (~ 1 m long).

Addition of xenon

The xenon used was of 99.995% purity (Air Products, Tamaqua, PA). The xenon gas flow was controlled with a needle valve. The xenon was conducted through a 1-m length of 0.32 cm i.d. Tygon tubing which was connected to a glass tee attached to the base of the ICP torch. A two-way switching valve was installed ahead of the needle valve so that the xenon flow could be conveniently turned off. This also facilitated measurement of the xenon flow rate with a soapfilm flowmeter (Alltech Model 4074, Deerfield, IL).

Solutions

Analyte solutions were prepared from 1000 mg L^{-1} standards from Fisher Scientific Co. (Fair Lawn, NJ). Ultrex II hydrochloric acid from J. T. Baker (Phillipsburg, NJ) was used to prepare a 1% HCl solution for the ClO^+ interference study. High purity deionized water (resistance ~ 18 MΩ) was obtained from a Barnstead Nanopure-II system (Newton, MA).

Instrumental conditions

General instrumental and sampling conditions are given in Table I. Intensities and isotope ratios were measured by peak hopping; spectra were obtained by scanning. A single set of experimental conditions was used for the determination of Si, V, Cr, and Fe. The determination of K required a higher xenon flow rate (37 mL min^{-1}) and a change in the potential of the photon stop. The resolution setting on the mass spectrometer was also increased to yield peaks ~ 0.5 amu wide at the base. At low resolution a steady signal could not be obtained at m/z = 41, perhaps due to overlap from the large Ar^+ peak at m/z = 40.

RESULTS AND DISCUSSION

Mass spectra

Figure 1 presents results for the silicon study. In the blank spectrum (Figure 1A) the polyatomic ions N_2^+ and N_2H^+ are below 200 counts s^{-1}, and NO^+ is under 1000 counts s^{-1} with xenon present. Table II shows the extent of the signal reduction with and without xenon in the ICP. The ions N_2^+ and N_2H^+ are attenuated by approximately a factor of 300, while NO^+ is reduced by a factor of 1400. A 5 mg L^{-1} Si solution gives well-resolved silicon peaks with a sensitivity of 55,000 counts s^{-1} per ppm for $^{28}Si^+$ (Figure 1B). Comparison of the analyte count rates (Table III) to the background count rates (Table II) shows that the ratio of residual background to analyte signal for 1 mg L^{-1} Si is 0.3% for $^{28}Si^+$ and 1.4% for $^{29}Si^+$ when Xe is added. However, the remaining peak from NO^+ is ~ 30% of the net signal for $^{30}Si^+$. Finally, the background from O_2^+ at m/z = 32 is of particular note. A large peak (~ 1 x 10^6 counts s^{-1}) remains even when xenon is added; a determination of sulfur at m/z = 32 is not facilitated by addition of xenon.

Results from the potassium study are depicted in Figure 2. Special experimental conditions were used for this element (Table I), notably a higher xenon flow rate and higher resolution. The residual background from ArH^+ at m/z = 41 is approximately 1300 counts s^{-1} (Figure 2A). A 10 mg L^{-1} K solution gives a net signal of 14,900

counts s^{-1} at m/z = 41 (Figure 2B and Table III). Thus, the ArH^+ peak still is a significant contribution (~ 9%) to the 10 mg L^{-1} K signal. The small background peak (~ 200 counts s^{-1}) at m/z = 39 in Figure 2A is probably from trace potassium in the water. Since there is little signal at m/z = 38 from $^{38}Ar^+$, $^{38}ArH^+$ is not the culprit. The addition of Xe and the use of higher resolution reduce the $^{40}Ar^+$ peak to ~ 15,000 counts s^{-1}. Thus, the contribution of $^{40}Ar^+$ to the background at m/z = 39 or 41 was largely eliminated.

The low level of ClO^+ when xenon is added is shown in Figure 3. The background for 1% HCl plus xenon shows five significant peaks in this region. From Table II the $^{35}ClO^+/^{37}ClO^+$ ratio is about 3:1, as expected from the natural abundances of the two chlorine isotopes. The background at m/z = 52 is likely a combination of $^{40}Ar^{12}C^+$ and $^{35}ClOH^+$, the former probably arising from carbon-containing impurities in the argon or the solvent. The peak at m/z = 54 is due to both $^{40}Ar^{14}N^+$ and $^{37}ClOH^+$. As shown in Tables II and III, residual backgrounds at m/z = 51 to 53 are less than 1% of the signals obtained for a solution containing V and Cr, each at 1 mg L^{-1}. However, the background at m/z = 54 is about 5% of the signal from $^{54}Cr^+$. The background at m/z = 53 is reduced by approximately a factor of 180, but that of m/z = 54 drops by only a factor of 45. Nonetheless, signals for the three chromium isotopes drop by only a factor of 7 (Table III) when Xe is added, much less than those of the background peaks. The background ion at m/z = 46 (probably NO_2^+) is also

attenuated substantially when Xe is added, although this reduction is hidden by the vertical scale in Figure 3B.

Results for iron are depicted in Figure 4. Addition of Xe attenuates the background ions ArN^+ at m/z = 54 and ArO^+ at m/z = 56 by factors of 200 and 170, respectively, as shown in Table II. In comparison, the $^{54}Fe^+$ signal from a 1 mg L^{-1} solution drops by only a factor of 16. The trend for the $^{56}Fe^+$ signal is similar, but the $^{56}Fe^+$ signal is 2.1 x 10^6 counts s^{-1} without Xe, and loss of detector gain at this high count rate may preclude a valid comparison (24). Figure 4A also shows that addition of xenon eliminates the common background peaks at m/z = 57 and 58, which would facilitate measurement of these minor isotopes of Fe.

Isotope ratios

The isotope ratios determined with added xenon are listed in Table IV. The ratios $^{28}Si/^{29}Si$, $^{53}Cr/^{52}Cr$, $^{54}Cr/^{52}Cr$, and $^{56}Fe/^{54}Fe$ agree well with the accepted natural abundance ratios. Thus, isotope ratios could be measured for these elements at ~ ppm levels (the usual levels used to obtain good precision) without background correction. However, the ratio $^{28}Si/^{30}Si$ differs markedly from the accepted value. This deviation is likely caused by the substantial NO^+ peak remaining at m/z = 30 relative to the signal from the minor isotope $^{30}Si^+$. Subtraction of the background signal at m/z = 30 does not improve the $^{28}Si/^{30}Si$ ratio very much (20.82 versus the accepted 29.75).

Correction for the background at m/z = 41 gives a $^{39}K/^{41}K$ ratio of 13.21, reasonably close to the accepted value of 13.86.

Detection limits

The detection limits (i.e., the solution concentration necessary to yield a net signal equivalent to three times the standard deviation of the background) for the five elements studied are listed in Table V. The major isotope of each element was used. These estimated detection limits are comparable to or slightly better than those observed for these elements if no special steps are taken to attenuate the polyatomic ions by addition of xenon.

Calibration curves

The linearity of calibration curves for Si, V, Cr, and Fe was tested with the addition of xenon. In each case the major isotope of each element was monitored. For Si, a series of six solutions from 0.01 mg L^{-1} to 10 mg L^{-1} yielded a calibration curve with a correlation coefficient of 0.9994. Curves from another series of six solutions containing 0.005 mg L^{-1} to 3 mg L^{-1} V, Cr, and Fe gave correlation coefficients of 0.9985, 0.9989, and 0.9992, respectively.

Effect of xenon on $ArCl^+$ and Ar_2^+

Further experiments were performed to determine whether added xenon would reduce $ArCl^+$ and Ar_2^+ and facilitate the determination of $^{75}As^+$ and $^{80}Se^+$. Instrumental conditions were matched as closely as

possible to those for Si, V, Cr, and Fe, as listed in Table I. A 1% HCl solution was used for background measurements. Figure 5A shows that xenon addition eliminates $ArCl^+$ and reduces Ar_2^+ by a factor of 3600 (Table II) to ~ 200 counts s^{-1}. However, Figure 5B shows that the nebulization of a 1% HCl solution containing As and Se under the same conditions gives a very low sensitivity: 890 counts s^{-1} per ppm for $^{75}As^+$ and 220 net counts s^{-1} per ppm for $^{80}Se^+$. These signals are approximately three orders of magnitude lower than those with argon only (Table III).

This observation that the reduction factors for As^+ and Se^+ are much greater than those for other analyte ions leads to a tentative explanation for the effect of added xenon. The first excited state of the neutral xenon atom is 8.31 eV above the ground state (26); the ionization energy of xenon is 12.1 eV. Both these values are ~ 3eV below the corresponding values for Ar, so the addition of small amounts of xenon would be expected to moderate ionization conditions in an Ar ICP. Elements which have IEs below ~ 8 eV (i.e., the energy corresponding to the first excited state of xenon) remain substantially ionized, which is the case for Si, K, V, Cr, and Fe. Elements which have an IE above ~ 8 eV such as As (IE = 9.81 eV) and Se (IE = 9.75 eV) are not ionized efficiently with xenon present. Most of the polyatomic species studied in this work have IEs at or above 11 eV (except for NO, 9.27 eV) (27). These more energetic polyatomic ions are attenuated greatly when xenon is added. The

fundamental reasons for the effect of xenon on background and analyte peaks are under investigation in our laboratory (28).

Effects of Xe on plasma structure and background

When yttrium is added as a test element, addition of small doses of xenon (10 or 37 mL min^{-1}) causes little visible change in the position of the red initial radiation zone or in the intensity of the blue emission from the normal analytical zone (29). Thus, there is no obvious, drastic change in the characteristics of the ICP when xenon is added.

The background at m/z values devoid of ions is very low (< 5 counts s^{-1}) when xenon is added. An example is shown at m/z = 74 in Figure 5A. Without xenon, the background is usually 30 counts s^{-1} for the operating conditions listed in Table I with this particular instrument. With xenon present, Xe^+ was a major background ion, the signal at m/z = 136 (8.9% abundance) being 1.8×10^6 counts s^{-1}. The total count rate for all Xe^+ peaks was ~ 2×10^7 counts s^{-1}. Thus, "matrix" suppression (30) caused by Xe^+ is also a likely source of loss of ions (28).

The Xe^+ peaks overlap or are adjacent to isotopes of Te, Cs, and Ba, so xenon should not be added when determining these elements. Polyatomic ions containing Xe, such as XeH^+, XeO^+, $XeAr^+$, $NaXe^+$ (from a 100 mg L^{-1} Na solution) or Xe_2^+ were not observed.

Comparison of Xe-Ar ICP with other plasmas

A rigorous comparison of the performance of mixed-gas Ar-N_2 ICPs (16-19) and the He microwave-induced plasma (MIP) (31) with that of the Ar-Xe ICP is complicated by several factors. The various investigators employ different nebulizers and desolvation methods, the count rates for analyte and polyatomic ions are sensitive to plasma operating conditions (particularly aerosol gas flow rate), and the criteria chosen for evaluating the potential improvements also differ. For these reasons, the relative merits of these schemes for reducing polyatomic ion interferences will be compared only in general terms and for those operating conditions that yield optimum performance.

Compared to the present work, addition of N_2 to the outer gas does not reduce levels of ArO^+, $ArOH^+$ and ClO^+ as extensively. However, analyte signals remain similar or can even be enhanced if the aerosol gas flow rate is reoptimized after the N_2 is added. Addition of N_2 also attenuates metal oxide ions substantially. The one case that can be compared fairly is that involving $^{56}Fe^+$ and $^{40}Ar^{16}O^+$. With addition of 8-20% N_2 into the outer gas, the background equivalent concentration (BEC) for Fe at m/z = 56 is 7 $\mu g\ L^{-1}$ without desolvation (17) and 0.6 $\mu g\ L^{-1}$ with desolvation (18). A pneumatic nebulizer was used in both these studies. In the present work, the BEC for Fe at m/z = 56 is 3 $\mu g\ L^{-1}$; a more efficient ultrasonic nebulizer with desolvation was used. The background (i.e., the "baseline" under all the peaks) stays about the same when N_2 is added to the outer gas, whereas addition of Xe reduces the background.

Incorporation of N_2 at a very low flow rate (30 mL min^{-1}) into the aerosol gas flow reduces In^+ signal by a factor of four. The ratio (In^+ signal)/(polyatomic ion signal) is improved by factors of two to 200 for many species. Unfortunately, the effect of adding N_2 to the aerosol gas on count rates for analyte ions of moderate to high ionization energy is not reported, although the accuracy obtained for As and Se at 100 $\mu g\ L^{-1}$ in 1% to 8% aqueous HCl is improved substantially with N_2 present (16). Compared to Xe, modification of the ICP with N_2 is attractive because analyte signals are higher and N_2 is much less expensive. However, polyatomic ions containing N are enhanced when N_2 is added (16-18), as expected from the initial ICP-MS study with Ar-N_2 plasmas (32). Thus, addition of N_2 compromises determination of Si and ^{54}Fe. The Ar-Xe plasma described in the present work is superior for applications involving these ions, particularly for isotope ratio experiments where the sacrifice in Si^+ and Fe^+ signal is not a big problem if sufficient amounts of these elements are available.

Caruso and co-workers have reported the only MS experiments with a He MIP into which the sample is introduced as an aqueous aerosol. N_2^+ and Ar^+ are major ions, and ArN^+ and ArO^+ are still observed. In fact, N_2^+ is actually added to this plasma to suppress Kr^+ and improve the linear dynamic range. Addition of N_2 enhances the peaks from the usual N-containing ions and also elevates the peak at m/z = 56, presumably due to formation of N_4^+ (31). Although the concept of a He plasma, either an MIP or an ICP (33), for MS is potentially

attractive, a viable system for routine analysis of solutions has not yet been demonstrated.

CONCLUSION

The addition of small amounts of xenon into the central channel of the ICP can greatly reduce the signal from various troublesome polyatomic ions. However, substantial analyte signal remains only if the analyte ionization energy is below the energy of the first excited states of xenon. Clearly, fundamental studies need to be performed on the effects of xenon introduction, including elucidation of any changes in temperatures in the ICP or possible matrix effects caused by the addition of Xe^+ to the ion beam.

LITERATURE CITED

1. Houk, R. S.; Fassel, V. A.; Flesch, G. D.; Svec, H. J.; Gray, A. L.; Taylor, C. E. Anal. Chem. 1980, 52, 2283.
2. Douglas, D. J.; Houk, R. S. Prog. Anal. At. Spectrosc. 1985, 8, 1.
3. Houk, R. S. Anal. Chem. 1986, 58, 97A.
4. Houk, R. S.; Thompson, J. J. Mass Spectrom. Rev. 1988, 7, 425.
5. Vaughan, M. A.; Horlick, G. Appl. Spectrosc. 1986, 4, 434.
6. Tan, S. H.; Horlick, G. Appl. Spectrosc. 1986, 4, 445.
7. Date, A. R.; Cheung, Y. Y.; Stuart, M. E. Spectrochim. Acta, Part B 1987, 42B, 3.
8. Hutton, R. C.; Eaton, A. N. J. Anal. At. Spectrom. 1987, 2, 595.
9. Zhu, G.; Browner, R. F. J. Anal. At. Spectrom. 1988, 3, 781.
10. Powell, M. J.; Boomer, D. W.; McVicars, R. J. Anal. Chem. 1986, 58, 2864.
11. Whittaker, P. G.; Lind, T.; Williams, J. G.; Gray, A. L. Analyst 1989, 114, 675.
12. Creed, J. T.; Davidson, T. M.; Shen, W. L.; Brown, P. G.; Caruso, J. A. Spectrochim. Acta, Part B 1989, 44B, 909.
13. Montaser, A.; Chan, S.-K.; Koppenaal, D. Anal. Chem. 1987, 59, 1240.
14. Bradshaw, N.; Hall, E. F. H.; Sanderson, N. E. J. Anal. At. Spectrom. 1989, 4, 801.
15. Rowan, J. T.; Houk, R. S. Appl. Spectrosc. 1989, 6, 976.

16. Evans, E. H.; Ebdon, L. J. Anal. At. Spectrom. 1989, 4, 299; 1990, 5, 425.

17. Lam, J. W. H.; Horlick, G. Spectrochim Acta, Part B 1990, 45B, 1313, 1327.

18. Lam, J. W. H.; McLaren, J. W. J. Anal. At. Spectrom. 1990, 5, 419.

19. McLaren, J. W.; Lam, J. W. H.; Gustavsson, A. Spectrochim. Acta, Part B 1990, 45B, 1091.

20. Montaser, A.; Van Hoven, R. L. CRC Crit. Rev. Anal. Chem. 1987, 18, 45.

21. Olson, K. W.; Haas, W. J., Jr.; Fassel, V. A. Anal. Chem. 1977, 49, 632.

22. Bear, B. R.; Fassel, V. A. Spectrochim. Acta, Part B 1986, 41B, 1089.

23. Scott, R. H.; Fassel, V. A.; Kniseley, R. N.; Dixon, D. E. Anal. Chem. 1974, 46, 75.

24. Kurz, E. A. Am. Lab. March 1979, 11, 67.

25. Weast, R. C., Ed. CRC Handbook of Chemistry and Physics; CRC Press, Inc.: Boca Raton, 1985-86; p B-238.

26. Moore, Charlotte E. Atomic Energy Levels, Vol. III; U.S. Government Printing Office: Washington, D.C., 1958; p 114.

27. Rosenstock, H. M.; Draxl, K.; Steiner, B. W.; Herron, J. T. Journal of Physical and Chemical Reference Data: Energetics of Gaseous Ions, Vol. 6, Supplement No. 1; National Bureau of Standards: Washington, D.C., 1977.

28. Smith, F. G.; Houk, R. S. unpublished results.

29. Koirtyohann, S. R.; Jones, J. S.; Yates, D. A. Anal. Chem. 1980, 52, 1965.

30. Gillson, G. R.; Douglas, D. J.; Fulford, J. E.; Halligan, K. W.; Tanner, S. D. Anal. Chem. 1988, 60, 1472.

31. Creed, J. T.; Davidson, T. M.; Shen, W.-L.; Brown, P. G.; Caruso, J. A. Spectrochim. Acta, Part B 1989, 44B, 909.

32. Houk, R. S.; Montaser, A.; Fassel, V. A. Appl. Spectrosc. 1983, 37, 425.

33. Montaser, A.; Chan, S.-K.; Koppenaal, D. W. Anal. Chem. 1987, 59, 1240.

Table I. Operating conditions

ICP torch	Ames Laboratory design (23)
	Outer tube extended 30 mm from middle tubes
Forward power	1.25 kW[a]
Argon flow rates (L min^{-1}):	
outer gas	13
auxiliary gas	0.2[a]
aerosol gas	1.55-1.60[a]
Xenon flow rates (mL min^{-1}):	
For Si, V, Cr, Fe	10
For K	37
Sampling position	22 mm from load coil[a], on center
Sampler	Copper, 1.1 mm diam. orifice
Skimmer	Nickel, 0.9 mm diam. orifice
Ions lens settings:	
Bessel box barrel	+5.4 V
Bessel box plate lens	-11.0 V
Einzel lenses 1 and 3	-19.8 V
Einzel lens 2	-130 V
Bessel box stop	-5.8 V: Si, V, Cr, Fe. -4.9 V: K.
Electron multiplier voltage	-3.4 kV: Si, V, Cr, Fe. -3.0 kV: K.

Table I. (continued)

Operating pressures:	
interface	1 torr
quadrupole chamber	3×10^{-5}
Spectral measurements:	Sequential monitoring mode
For Si, V, Cr, Fe	Low resolution, 10 measurements per peak
	Measurement time = 1.0 s
For K	High resolution, 20 measurements per peak
	Measurement time = 0.25 s
All other measurements:	Multielement monitoring mode (peak hopping)
For Si, V, Cr, Fe	Low resolution, 3 measurements per peak
	Dwell time = 10 ms
	Total measurement time = 1.0 s
For K	High resolution, 3 measurements per peak
	Dwell time = 10 ms
	Total measurement time = 1.0 s

[a]Typical values for these conditions. There was some variation between experiments conducted on different days.

Table II. Background count rates

m/z	ion(s)	Ar only counts s^{-1} mean[a]	Xe added counts s^{-1} mean[a]	Reduction factor
28	N_2^+	50,600	165	300
29	HN_2^+	13,100	40	325
30	NO^+	1.1×10^6	780	1400
40	Ar^+	throttled[b]	14,500[c]	---
41	ArH^+	throttled[b]	1300[c]	---
51	$^{35}ClO^+$	24,000[d]	140	170
52	ArC^+, $^{35}ClOH^+$	8,600[d]	670	13
53	$^{37}ClO^+$	7,990[d]	45	180
54	ArN^+, $^{37}ClOH^+$	9,970[d]	230	45
54	ArN^+	14,100	70	200
56	ArO^+	72,800	430	170
75	$^{40}Ar^{35}Cl^+$	890	7	125
80	$^{40}Ar_2^+$	726,000	200	3600

[a]Mean of 20 measurements.

[b]Total count rate above 3.2×10^6 counts s^{-1}; instrument throttled or shutdown.

[c]Higher Xe flow rate and resolution were used (see Table I).

[d]Count rate obtained during introduction of 1% HCl.

Table III. Net analyte count rates

ion(s)	Ar only counts s^{-1} per ppm[a]	Xe added counts s^{-1} per ppm[a]	Reduction factor
$^{28}Si^+$	550,000	55,000	10
$^{29}Si^+$	18,600	2,870	6
$^{30}Si^+$	throttled[b]	2,640	-
$^{39}K^+$	510,000	19,700[c]	26
$^{41}K^+$	throttled[b]	1,490[c]	-
$^{51}V^+$	$1.5x10^6$	207,000	7
$^{52}Cr^+$	$1.2x10^6$	163,000	7
$^{53}Cr^+$	129,000	18,500	7
$^{54}Cr^+$	32,500	4,800	7
$^{54}Fe^+$	139,000	8,800	16
$^{56}Fe^+$	$2.1x10^6$	139,000	15
$^{75}As^+$	653,000	890	730
$^{80}Se^+$	528,000	220	2400

[a]Mean of 20 measurements.

[b]Total count rate above 3.2×10^6 counts s^{-1}; instrument throttled or shutdown.

[c]Higher Xe flow rate and resolution were used (see Table I).

Table IV. Isotope ratio measurements with Xe added

Solution conc. (mg L^{-1})	Ratio Measured	Determined Ratio mean	RSD(%)[a]	Accepted Ratio (25)
5	$^{28}Si/^{29}Si$	19.10	0.8	19.75
5	$^{28}Si/^{30}Si$	20.82[b]	1.6	29.75
10	$^{39}K/^{41}K$	13.21[b]	1.0	13.86
1	$^{53}Cr/^{52}Cr$	0.1135	0.7	0.1134
1	$^{54}Cr/^{52}Cr$	0.0294	1.4	0.0282
1	$^{56}Fe/^{54}Fe$	15.78	0.6	15.81

[a]Mean and relative standard deviation of 20 measurements.

[b]Count rates for $^{30}Si^+$ and $^{41}K^+$ were corrected for contributions from NO^+ and ArH^+.

Table V. Estimated detection limits

Element	m/z	Detection Limit ($\mu g\ L^{-1}$)
Si	28	0.6
K	39	1
V[a]	51	0.3
Cr[a]	52	2
Fe[a]	56	0.3

[a]In 1% HCl solution.

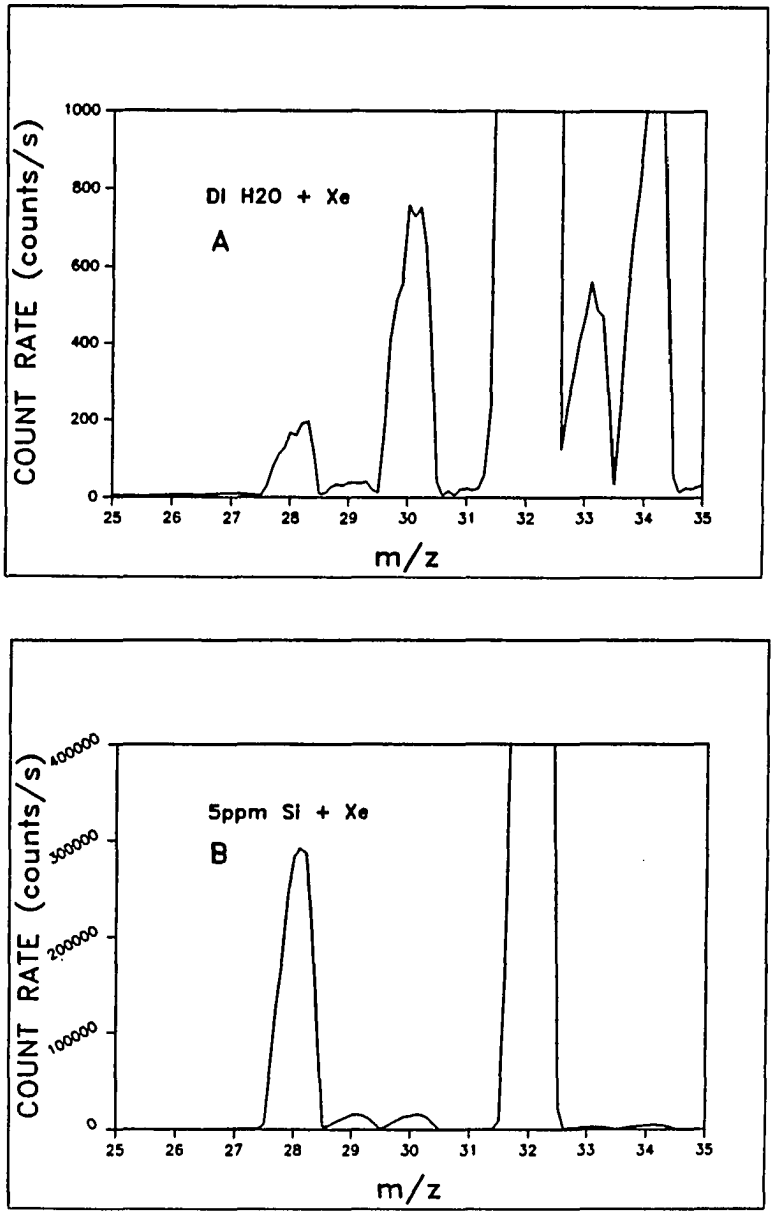

Figure 1. Spectra of (A) deionized water plus 10 mL min^{-1} Xe and (B) 5 mg L^{-1} Si plus 10 mL min^{-1} Xe

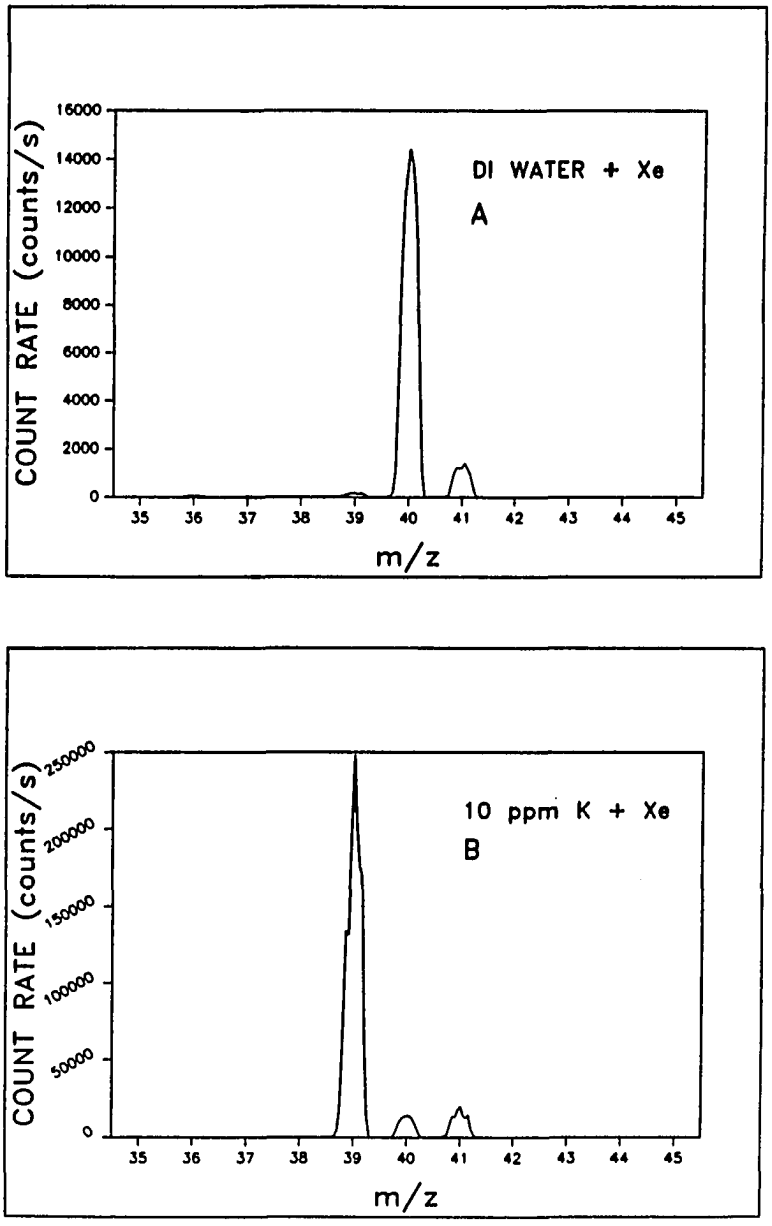

Figure 2. Spectra of (A) deionized water plus 37 mL min^{-1} Xe and (B) 10 mg L^{-1} K plus 37 mL min^{-1} Xe; resolution switched to high

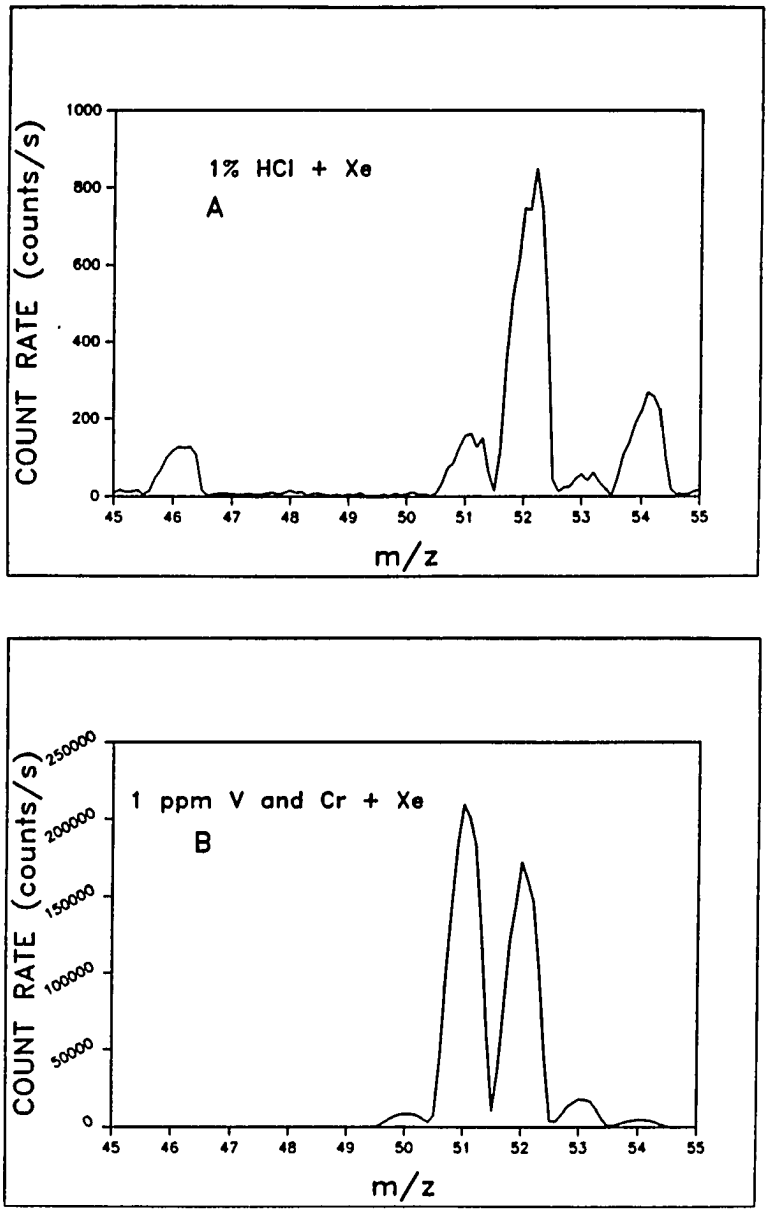

Figure 3. Spectra of (A) 1% HCl plus 10 mL min^{-1} Xe and (B) 1 mg L^{-1} V and Cr in 1% HCl plus 10 mL min^{-1} Xe

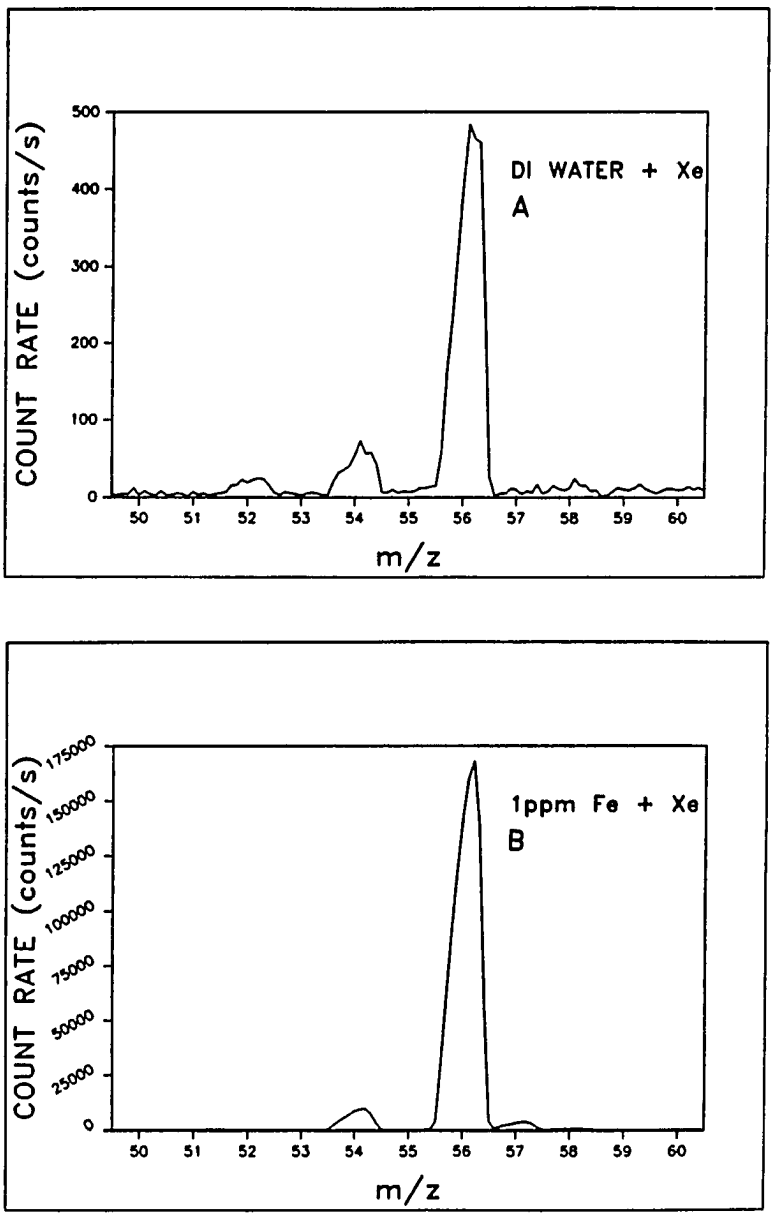

Figure 4. Spectra of (A) deionized water plus 10 mL min^{-1} Xe and (B) 1 mg L^{-1} Fe plus 10 mL min^{-1} Xe

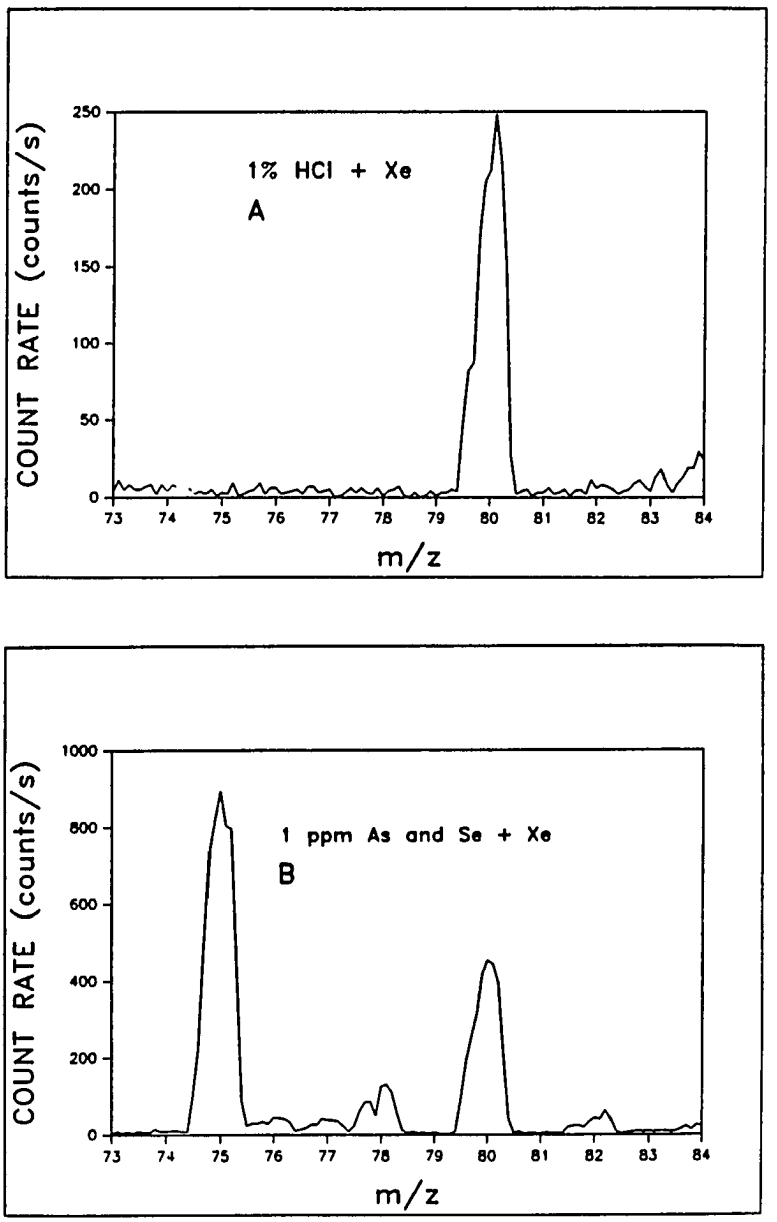

Figure 5. Spectra of (A) 1% HCl plus 10 mL min^{-1} Xe and (B) 1 mg L^{-1} As and Se plus 10 mL min^{-1} Xe

SECTION IV.

TEMPERATURE AND ELECTRON DENSITY MEASUREMENTS AND MATRIX EFFECT STUDIES OF AN ARGON-XENON PLASMA FOR INDUCTIVELY COUPLED PLASMA MASS SPECTROMETRY

INTRODUCTION

Previous work by the authors demonstrates that addition of xenon to the central channel of an argon inductively coupled plasma (ICP) markedly reduces the count rates of various polyatomic ion interferences (N_2^+, N_2H^+, NO^+, ArH^+, ClO^+, ArC^+, $ClOH^+$, ArN^+, ArO^+) observed in ICP-mass spectrometry (MS) (1). Alleviation of these interferences allows the measurement of atomic ion signals and isotope ratios for Si, K, V, Cr, and Fe with little or no background correction. These measurements are possible because the ion signals for the interfering ions drop more sharply than those for the analytes. A possible explanation for this effect is the focus of this paper.

Temperatures and electron density (n_e) are important fundamental parameters of a plasma. Knowledge of these parameters may help explain the effects of added xenon and provide insights on how to improve the performance of the technique.

Two important plasma temperatures are the ionization temperature (T_{ion}) and the excitation temperature (T_{exc}). T_{ion} describes the extent of ion formation in the ICP. This temperature may be determined via the Saha equation by measurement of the relative intensities of atom and ion emission lines of a suitable species if n_e is also known (2-4). T_{ion} can also be determined by ICP-MS, where the count rate ratio from ions of two elements close in mass but far

different in ionization energy (IE) (e.g., Ga and As) is measured; T_{ion} is again calculated by the Saha equation with a value of n_e (5,6). T_{exc} describes the population density of electronically excited states. In thermal equilibrium this population density follows a Boltzmann distribution, so the emission intensity from a higher energy level to a lower one is a function of the excitation energy, the transition probability, and T_{exc} (3, 7-9).

The electron density can be measured by a number of different techniques (10). The Stark broadening method is common (11-14). A spectral line is broadened due to the interaction of an emitting atom with the static electric field generated by the surrounding ions and electrons in the plasma. The H_β line (486.13 nm) is used as it is a strong line which exhibits substantial Stark broadening. Nonetheless, contributions from instrumental and Doppler broadening must be deconvoluted from the experimental line profile to obtain an accurate n_e.

One other aspect for study is the so-called "matrix effect" in ICP-MS. Generally, the analyte ion signal in ICP-MS is suppressed in the presence of a matrix element (15-17). Various theories have been set forth to explain this effect. These include diffusion effects in the ICP (18), collisional and mass enrichment effects during ion extraction (19,20), and space charge repulsions in the ion beam (21). In any case, matrix interferences have been found to depend on ICP-MS operating conditions and on the measured ionization energies of the elements in question (22).

This paper describes the measurement of temperatures and n_e with addition of xenon and krypton and introduction of a cesium matrix to the ICP. Matrix effects induced by adding an inert gas (e.g., Xe) are compared to those caused when an element of similar mass (Cs) is added from a nebulized solution in sufficient quantity to yield similar count rates for a particular analyte. Results are also described for an analogous experiment with Kr and Rb. Finally, the effects of added Xe and Kr on polyatomic ion and analyte ion signals are compared.

EXPERIMENTAL

Instrumentation

The inductively coupled plasma mass spectrometer used was the ELAN Model 250 with upgraded ion optics (Perkin-Elmer SCIEX, Thornhill, Ontario, Canada). The center section of the shielding box surrounding the ICP-MS interface was removed to allow optical emission measurements from the ICP. As shown in Figure 1, the emission was focused by a Pyrex lens (5 cm diam., f/2, magnification 1.6) onto the entrance of a fiber optic cable from C. Technologies, Inc. (Short Hills, NJ). The fiber optic cable was ~ 21 m long with a 600 μm diameter fused silica core surrounded by a doped fused silica cladding. Emission from the cable was focused onto the entrance slit of the monochromator described in Table I.

Sample solutions were introduced to the ICP by an ultrasonic nebulizer (Model U-5000, Cetac Technologies, Inc., Omaha, NE) with a solution uptake rate of 3.0 mL min^{-1}. The heating chamber of the desolvator was set at 140 ^{o}C, and the condenser was operated at 0 ^{o}C. The resulting dry aerosol was transported to the plasma through 0.48 cm i.d. Tygon tubing.

Operating conditions

Operating conditions for the monochromator and the ICP-MS device are given in Tables I and II, respectively. Changes in certain

parameters for different experiments are noted, specifically the holographic grating for the monochromator, the exposure time and number of integrations for the photodiode array, and the voltage on the Channeltron electron multiplier of the ICP-MS instrument.

Addition of Xe and Kr

The xenon (Spectra Gases, Newark, NJ) and krypton (Air Products, Tamaqua, PA) were specified to be 99.995% pure. The gases were introduced and the flow rates measured as previously described (1), except that each gas was conducted through a much thinner tube (~ 1 mm i.d. Tygon, 1 m long). This facilitated rapid changing and purging of each gas and much faster (30 s) equilibration of the ion signal. As shown in Figure 1, a 23 gauge needle (0.64 mm o.d.) was placed in one end of the tubing, and the needle was inserted into a rubber septum connected to a glass tee attached to the base of the ICP torch. To switch from one gas to the other, the small 100-L tanks of Xe or Kr were simply disconnected from the regulator.

Solutions

Analyte solutions were prepared from 1000 mg L^{-1} standards from Plasmachem Associates, Inc. (Bradley Beach, NJ). The Cs and Rb matrix elements, also from Plasmachem, were prepared from the nitrates, so ClO^+ was avoided. A 100 mg L^{-1} Fe solution for the T_{exc} study was prepared from $FeCl_3 \cdot 6H_2O$ from Fisher Scientific Co. (Fair Lawn, NJ). Ultrex II hydrochloric acid from J. T. Baker (Phillipsburgh, NJ) was

used to prepare a 1% HCl solution for the measurement of ClO^+. High purity deionized water (resistance ~ 18 MΩ) was obtained from a Barnstead Nanopure-II system (Newton, MA).

Electron density measurements

The electron density was measured via the Stark broadening method using the H_β line at 486.13 nm (11-14). Emission was monitored from the central channel of the ICP during ion extraction approximately 1 mm upstream of the tip of the sampler. The effective observation zone was an area 13 μm wide and 0.4 mm long centered just upstream of the orifice. Distilled, doubly deionized water (DDW) was introduced to the ICP to avoid any spectral interferences.

A window from 477 nm to 492 nm was monitored using a photodiode array as a detector. The wavelength scale of the array was calibrated by using the pixels corresponding to maximum intensity of the Ar I emission lines at 487.63 nm and 488.79 nm. The width of each pixel was calculated to be 0.01183 nm. First, a profile of the dark current from the photodiode array was taken. Experimental H_β profiles were then taken at Xe and Kr flow rates of 0, 1, 2, 5, 10, and 20 mL min^{-1}, and each profile corrected for dark current was stored in the computer described in Table I. Abel inversion was not performed on these profiles, as previous work has shown that the full width at half maximum of the H_β emission from just in front of the sampler is not significantly different from the center of the ICP versus a lateral measurement (25). No self-reversal of the H_β line was observed.

After collection of the experimental profiles, an instrumental profile was collected to correct for instrumental broadening. This profile was obtained with the Fe I 485.97 nm line emitted from an iron hollow cathode lamp (Hamamatsu Photonics K.K., Japan) operated at a current of 20 mA. Again, the profile was first corrected for dark current.

The experimental and instrumental profiles were entered into a computer program developed by Chan and Montaser (14). A Doppler profile to correct for Doppler broadening was generated using a translational temperature (T_{tran}) of 5000 K. The program determined n_e by least-squares curve fittings of the H_β line to the theoretical Stark-broadened profiles.

Excitation temperature measurements

The excitation temperature was determined by measuring net intensities for seven Fe I lines between 370 nm and 377 nm, as described by Blades and Caughlin (26). All profiles were corrected for dark current. The linear regression of $\ln(I(\lambda_{qp})^3/g_q f_{pq})$ versus E_q (a Boltzmann plot) gives a slope of $-(kT)^{-1}$, where I is the emission intensity for each line, λ_{qp} is the wavelength, g_q is the degeneracy of the upper level, f_{pq} is the oscillator strength, E_q is the excitation energy, k is the Boltzmann constant (0.6952 cm^{-1}/K), and T is the excitation temperature. Wavelengths, the factor $(\lambda_{qp})^3/g_q f_{pq}$, and the excitation energies are listed in Table III.

T_{exc} was calculated for the same xenon flow rates as for the n_e measurements.

Ionization temperature measurements

The ionization temperature was measured by MS with three thermometric pairs of elements: Ga and As, In and Sb, and In and Pd. The elements in each pair are close in mass but quite different in ionization energy (IE). Therefore, ion transmission through the mass spectrometer should be similar for the elements in each pair, giving an accurate measurement of T_{ion}. T_{ion} measured via Pd/In was of special interest as the IE of Pd (8.33 eV) is very close to the energy of the first excited state of Xe (8.31 eV). Signals for elements with IEs above the energy of this Xe state are lost drastically with addition of Xe, as is the case for As and Se (1).

Solutions containing 2 mg L^{-1} Ga and As and 1 mg L^{-1} In, Pd, and Sb were introduced to the ICP. The element of lower ionization energy was used as the reference for isotope ratio measurements. The following ratios were measured at previously listed Xe and Kr flow rates: $^{71}Ga/^{69}Ga$, $^{75}As/^{69}Ga$, $^{121}Sb/^{115}In$, and $^{105}Pd/^{115}In$. Data acquisition parameters for the isotope ratio measurements are listed in Table II. Relative standard deviations (RSDs) for the ratios ranged from 0.2% to 5.0%, with worse precision due to signal loss at higher Xe and Kr flow rates.

The measured ratios were corrected for differences in the molarity and isotopic abundance of each element in solution, and the corrected

ratios were entered into appropriate FORTRAN computer programs. These programs are named TCALCAS, TCALCSB, and TCALCPD, the latter based on the former two programs (28). In these programs partition functions for the reference elements (Ga or In) and the thermometric elements (As, Pd, or Sb) are calculated at an arbitrary starting temperature (7000 K) (29,30). At a measured n_e, the degree of ionization (α) is calculated for the reference element via the Saha equation, and α for the thermometric element is calculated by the relative degree of ionization for the thermometric pair. A value of T_{ion} is calculated using α of the thermometric element in the Saha equation, and the procedure is iterated until T_{ion} converges to within 0.1% of its previous value. The random error estimated for the T_{ion} measurements is ~ 0.4% RSD.

Matrix-matching study

For this study the ion signal from a 1.0 mg L^{-1} V solution with addition of Xe or Kr was compared to the ion signal from the same concentration of V with an added matrix element. To minimize mass discrimination effects (31-34), Rb was chosen to mimic the effects of Kr, and Cs was chosen for Xe. The electron multiplier voltage was lowered considerably (-2900 V) so the ion signal for V would remain near 1 x 10^6 counts s^{-1}, avoiding loss of detector gain (35).

Matrix solutions contained 10, 30, 50, or 100 mg L^{-1} of Rb or Cs. Solutions containing 100 mg L^{-1} Rb and Cs were checked for an elevated background from ClO^+ at m/z = 51, but this amounted to only ~ 100

counts s^{-1}. The electron density was also measured when 100 mg L^{-1} Cs was introduced to the ICP.

Another experiment was performed to investigate any effects of a matrix on T_{ion} measurements. Solutions containing 2 mg L^{-1} Ga and As and 1 mg L^{-1} Pd, In, and Sb were prepared in 10, 30, 50, and 100 mg L^{-1} Cs. The isotope ratios described previously were measured and entered into the programs TCALCAS, TCALCSB, or TCALCPD with an appropriate n_e.

Xe vs Kr study

Addition of xenon to the ICP was compared to addition of krypton for reduction of interfering ion and analyte ion signal. Flow rates for each gas were 0 and 10 mL min^{-1}. Experimental conditions were reproduced as close as possible to the previous xenon study (1). However, due to the higher sensitivity obtained with the commercial ultrasonic nebulizer used in this work, lower analyte concentrations (0.5 mg L^{-1} Si, 0.1 mg L^{-1} V, Cr, and Fe) were used.

RESULTS AND DISCUSSION

Electron density measurements

The n_e values were measured in the gas directly in front of the sampling orifice. With addition of xenon, n_e ranged from 9.4 x 10^{14} cm^{-3} at 20 mL min^{-1} Xe to 1.0 x 10^{15} cm^{-3} at 2, 5, and 10 mL min^{-1} Xe. The bottom flow rates of 0 and 1 mL min^{-1} Xe each yielded an n_e of 9.9 x 10^{14} cm^{-3}. The results for addition of krypton and introduction of 100 mg L^{-1} Cs were also in the above range (9-10 x 10^{14} cm^{-3}). Therefore, n_e varies at most by only ~ 5% from an overall mean value of 9.9 x 10^{14} cm^{-3}. The RSD of all measurements is $\pm$2.2%, so at 2σ (95% confidence interval) the RSD is $\pm$4.4%, indicating no substantial change in n_e in front of the sampler with addition of Xe, Kr, or Cs. These n_e values are quite close to various literature values (14,25,26).

Plasma temperature measurements

Results for T_{exc} measurements with addition of xenon are presented in Table IV. A gradual increase (~ 200 K) in T_{exc} with increasing Xe flow rate is indicated, but this increase is well within the uncertainties of the individual measurements, estimated from the standard deviations of the slopes of the Boltzmann plots. The mean value of T_{exc} is ~ 4800 K, which is in good agreement with the value reported by Blades (26) but approximately 1000 K lower than other

literature values (3,7,11,36). Correlation coefficients for the plots range from 0.9881 to 0.9931. Thus, addition of xenon does not greatly affect T_{exc} in the gas flowing into the sampler. This agrees with the observation that the ICP does not change visibly when a small amount of Xe ($\leq$ 20 mL min^{-1}) is added (1).

Variation in T_{ion} with addition of xenon is shown in Figure 2. For the thermometric pairs $^{75}As/^{69}Ga$ and $^{121}Sb/^{115}In$ T_{ion} drops by ~ 400 K, the most noticeable reduction occurring with the addition of 1 to 2 mL min^{-1} Xe. However, the T_{ion} for the pair $^{105}Pd/^{115}In$ is substantially higher than the other pairs, with a gradual rise in T_{ion} observed at higher flow rates. This behavior may be due to the proximity of the IE of Pd (8.33 eV) and the energy of the first excited state of Xe (8.31 eV). Perhaps Penning ionization reactions between excited Xe atoms and Pd produce enough Pd ions so the $^{105}Pd/^{115}In$ ion signal ratio and thus T_{ion} remain relatively constant. The ratio $^{69}Ga/^{71}Ga$ was also monitored over all Xe flow rates, and the measured ratio was distributed evenly about the mean of 1.581 (RSD = 1.8%). This compares well with the natural abundance ratio of 1.532, indicating no significant change in $^{69}Ga/^{71}Ga$ as Xe was added that could bias T_{ion}.

Little change was observed in T_{ion} with addition of krypton, as depicted in Figure 3. This experiment was performed on a different day from Figure 2, and T_{ion} is different with and without Kr. The first excited state of Kr occurs at 9.91 eV, and since all the elements in the pairs have IEs below this energy, the respective ion

signal ratios and T_{ion}s are not greatly affected. Figure 4 shows that introduction of 10 to 30 mg L^{-1} Cs causes a modest rise in T_{ion} (~ 100 K) but this increase levels off at higher Cs concentrations. A T_{ion} for the $^{105}Pd/^{115}In$ ratio was not obtained as the measured ratios were all above one.

Matrix-matching study

The ion signals for 1.0 mg L^{-1} V with and without 1 mL min^{-1} Xe and with various concentrations of Cs are tabulated in Table V. The signal suppression from addition of xenon is most closely matched at a Cs concentration from 30 mg L^{-1} to 50 mg L^{-1} Cs. As shown in Table VI, the suppression of V signal by 2 mL min^{-1} Kr is most closely matched by 10 mg L^{-1} Rb.

An attempt to match the total number of Kr or Xe ions with the total number or Rb or Cs ions was not successful. A linear calibration curve for the Rb and Cs matrix solutions could not be obtained, despite the use of low detector voltages and the OmniRange utility on the SCIEX ICP-MS device. A possible reason for this behavior may be severe space charge effects on the extracted ion beam at the higher Rb and Cs concentrations (21).

Xe vs Kr study

A comparison of polyatomic ion loss with addition of Kr or Xe is presented in Table VII. Xenon clearly reduces these ions to a greater extent; addition of Kr exhibits reduction factors of only 1 to 4 while

addition of Xe shows reduction factors of 3 to 160. The count rates of these ions and the reduction factors are lower than those of the original xenon study (1), and this is most likely due to the different ultrasonic nebulizer used and differences in experimental conditions. However, the trend in reduction is similar, with the ions at m/z = 52 (ArC^+, $^{35}ClOH^+$) and m/z = 54 (ArN^+, $^{37}ClOH^+$) being the most difficult to attenuate. The one striking anomaly is the much lower reduction factor for NO^+ (60 in the present work vs. 1400) at m/z = 30; again, different operating conditions are probably the cause.

Analyte ion signal with and without added Kr or Xe is presented in Table VIII. Krypton reduces analyte signals by only a factor of three, but reduction factors range from 15 to 60 with added Xe. These reduction factors with Xe are greater than those reported previously (1), but analyte ion signals per ppm are still substantial. Furthermore, the polyatomic ion signals still drop more sharply than that of the analytes, except for the $ClOH^+$ ions.

CONCLUSION

Results provide evidence that signal loss for analytes of low IE (< 8eV) when Xe or Kr is added to the ICP is largely due to a matrix effect since this loss can be mimicked by introduction of enough matrix element of similar mass. Krypton results show that matrix effects also occur for polyatomic ions. Preferential loss of polyatomic ions versus analyte ions may be caused by the lowered T_{ion} induced by addition of Xe. Indeed, Kr does not appreciably change T_{ion} and attenuates polyatomic ion and analyte ion signals to a much lesser degree.

LITERATURE CITED

1. Smith, F. G.; Wiederin, D. R.; Houk, R. S. submitted for publication in Anal. Chem.
2. Griem, H. R. Plasma Spectroscopy; McGraw-Hill: New York, 1964; p. 119.
3. Adler, J. F.; Bombelka, R. M.; Kirkbright, G. F. Spectrochim. Acta, Part B 1980, 35B, 163.
4. Furuta, N. Spectrochim. Acta, Part B 1985, 40B, 1013.
5. Houk, R. S.; Svec, H. J.; Fassel, V. A. Appl. Spectrosc. 1981, 35, 380.
6. Houk, R. S.; Montaser, A.; Fassel, V. A. Appl. Spectrosc. 1983, 37, 425.
7. Kawaguchi, H.; Ito, T.; Mizuike, A. Spectrochim. Acta, Part B 1981, 36B, 615.
8. Furuta, N.; Horlick, G. Spectrochim. Acta, Part B 1982, 37B, 53.
9. Chan, S.-K.; Montaser, A. Spectrochim. Acta, Part B 1987, 42B, 591.
10. Hasegawa, T.; Haraguchi, H. In Inductively Coupled Plasmas in Analytical Atomic Spectrometry, 2nd ed.; Montaser, A.; Golightly, D. W., Eds.; VCH Press: New York, in press.
11. Kalnicky, D. J.; Fassel, V. A.; Kniseley, R. N. Appl. Spectrosc. 1977, 31, 137.
12. Goode, S. R.; Deavor, J. F. Spectrochim. Acta, Part B 1984, 39B, 813.

13. Caughlin, B. L.; Blades, M. W. Spectrochim. Acta, Part B 1985, 40B, 987.

14. Chan, S.-K.; Montaser, A. Spectrochim. Acta, Part B 1989, 44B, 175.

15. Houk, R. S.; Fassel, V. A.; Flesch, G. D.; Svec, H. J.; Gray, A. L.; Taylor, C. E. Anal. Chem. 1980, 52, 2283.

16. Date, A. R.; Gray, A. L. Analyst 1983, 108, 1033.

17. Olivares, J. A.; Houk, R. S. Anal. Chem. 1986, 58, 20.

18. Gregoire, D. C. Spectrochim. Acta, Part B 1987, 42B, 895.

19. Beauchemin, D.; McLaren, J. W.; Berman, S. S. Spectrochim. Acta, Part B 1987, 42B, 467.

20. Tan, S. H.; Horlick, G. J. Anal. At. Spectrom. 1987, 2, 745.

21. Gillson, G. R.; Douglas, D. J.; Fulford, J. E.; Halligan, K. W.; Tanner, S. D. Anal. Chem. 1988, 60, 1472.

22. Crain, J. S.; Smith, F. G.; Houk, R. S. Spectrochim. Acta, Part B 1988, 43B, 1355.

23. Winge, R. K.; Fassel, V. A.; Edelson, M. C. Spectrochim. Acta, Part B 1988, 43B, 85.

24. Scott, R. H.; Fassel, V. A.; Kniseley, R. N.; Nixon, D. E. Anal. Chem. 1974, 46, 75.

25. Crain, J. S.; Smith, F. G.; Houk, R. S. Spectrochim. Acta, Part B 1990, 45B, 249.

26. Blades, M. W.; Caughlin, B. L. Spectrochim. Acta, Part B 1985, 40B, 579.

27. Bridges, J. M.; Kornblith, R. L.; Astrophys. J. 1974, 192, 793.

28. Crain, J. S.; Ph.D. Dissertation, Iowa State University, 1989.

29. de Galan, L.; Smith, R.; Winefordner, J. D. Spectrochim. Acta, Part B 1968, 23B, 521.

30. Tamaki, S.; Kuroda, T. Spectrochim. Acta, Part B 1987, 42B, 49.

31. Russ, G. P. III; Bazan, J. M. Spectrochim. Acta, Part B 1987, 59, 984.

32. Ting, B. T. G.; Janghorbani, M. Spectrochim. Acta, Part B 1987, 42B, 21.

33. Houk, R. S.; Thompson, J. J. Mass Spectrom. Rev. 1988, 7, 425.

34. Russ, G. P. III; Bazan, J. M.; Date, A. R. Anal. Chem. 1987, 59, 984.

35. Kurz, E. A. Am. Lab. March 1979, 11, 67.

36. Faires, L. M.; Palmer, B. A.; Engelman, R., Jr.; Niemczyk, T. M. Spectrochim. Acta, Part B 1984, 39B, 819.

Table I. Instrumentation and operating conditions for AES measurements

Monochromator (23)	McPherson M2051, 1-m focal length.
	holographic grating
	1800 grooves mm^{-1} for $\lambda > 430$ nm
	3600 grooves mm^{-1} for $\lambda < 430$ nm
	entrance slit width = 20 μm
Detector	Princeton Applied Research, Model
	1453 photodiode array,
	unintensified, cooled to -15 ^{o}C
Computer	Princeton Applied Research Model 1461
	detector interface linked to DEC
	11/34 computer
Data acquisition	n_e measurements
	exposure time = 30 s
	integrations: 1
	T_{exc} measurements
	exposure time = 10 s
	integrations: 10

Table II. Operating conditions for SCIEX ICP-MS

ICP torch	Ames Laboratory design (24)
	Outer tube extended 30 mm from inner tubes
Forward power	1.25 kW
Argon flow rates (L min^{-1}):	
outer gas	13
auxiliary gas	0.2
aerosol gas	1.40
Sampling position	20 mm from load coil, on center
Sampler	Copper, 1.1 mm diam. orifice
Skimmer	Copper, 0.9 mm diam. orifice
Ion lens settings:	
Bessel box barrel	+5.4 V
Bessel box plate	-11.0 V
Einzel 1 and 3	-19.8 V
Einzel 2	-130 V
Bessel box stop	-4.9 V
Operating pressures	
interface	1 torr
quadrupole chamber	2×10^{-5} torr
Electron multiplier voltage	T_{ion} measurements: -2900 V
	matrix study: -2900 V
	Xe vs. Kr study: -3400 V

Table II. (continued)

Data acquisition	Measurement time = 1.0 s
	Dwell time = 10 ms
	Measurements per peak: 3
	Resolution: low

Table III. Fe I lines used for T_{exc} measurements (26)

Wavelength (nm)	$(\lambda_{qp})^3/g_q f_{pq}$ (27)	E_q (cm^{-1})
371.994	1.38550×10^{-13}	26875
372.256	9.82936×10^{-13}	27560
373.487	2.55167×10^{-14}	33695
373.713	1.93916×10^{-14}	27167
375.823	5.30828×10^{-14}	34329
376.379	8.25802×10^{-14}	34547
376.719	1.16964×10^{-13}	34692

Table IV. T_{exc} measurements with addition of Xe

Xe flow rate (mL min^{-1})	T_{exc} (K)[a]
0	4670 ± 320
1	4710 ± 350
2	4760 ± 340
5	4780 ± 320
10	4850 ± 300
20	4880 ± 270

[a] T_{exc} derived from slope of regression line of Boltzmann plot. Uncertainties are 1σ, estimated from error in slope.

Table V. Cs matrix-matching study

Xe flow rate (mL min^{-1})	Cs conc. (mg L^{-1})	Count rate for 1.0 mg L^{-1} V (counts s^{-1})[a]
0	0	1,540,000
1	-	138,500
-	10	359,800
-	30	155,300
-	50	112,600
-	100	43,100

[a]Mean of 20 measurements.

Table VI. Rb matrix-matching study

Kr flow rate (mL min^{-1})	Rb conc. (mg L^{-1})	Count rate for 1.0 mg L^{-1} V (counts s^{-1})[a]
0	0	1,633,000
2	-	1,198,000
-	10	1,148,000
-	30	613,000
-	50	505,400
-	100	479,400

[a]Mean of 20 measurements.

Table VII. Comparison of polyatomic ion loss for Kr and Xe addition

m/z	ion(s)	Counts s^{-1} no added Kr or Xe[a]	Counts s^{-1} Kr added[b]	Counts s^{-1} Xe added[b]	Reduction factor Kr	Reduction factor Xe
28	N_2^+	837,700	288,300	5,200	3	160
29	N_2H^+	198,500	53,280	1,520	4	130
30	NO^+	57,970	16,240	980	3.5	60
51	$^{35}ClO^+$	42,100[c]	27,300	1,900	1.5	22
52	ArC^+, $^{35}ClOH^+$	10,300[c]	7,720	3,400	1.3	3
53	$^{37}ClO^+$	14,100[c]	9,140	630	1.5	22
54	ArN^+, $^{37}ClOH^+$	3,190[c]	3,140	1,120	1	3
54	ArN^+	2,350	750	40	3	60
56	ArO^+	21,500	7,860	190	3	110

[a]Mean of 20 measurements.

[b]Mean of 20 measurements with 10 mL min^{-1} Kr or 10 mL min^{-1} Xe.

[c]Count rate obtained during introduction of 1% HCl. All other count rates were measured during introduction of DDW.

Table VIII. Comparison of net analyte count rates for Kr and Xe addition

ion(s)	Counts s^{-1} per 0.1 ppm no added Kr or Xe[a]	Counts s^{-1} per 0.1 ppm Kr added[b]	Counts s^{-1} per 0.1 ppm Xe added[b]	Reduction factor Kr	Reduction factor Xe
$^{28}Si^+$	485,000	164,000	8,140	3	60
$^{29}Si^+$	21,800	8,380	430	2.6	50
$^{30}Si^+$	12,760	5,100	310	2.5	40
$^{51}V^+$	312,500	112,000	16,460	3	19
$^{52}Cr^+$	192,000	67,800	12,900	3	15
$^{53}Cr^+$	21,900	7,700	1,430	3	15
$^{54}Cr^+$	5,290	1,850	260	3	20
$^{54}Fe^+$	19,900	7,520	1,200	2.6	17
$^{56}Fe^+$	339,000	116,800	19,100	3	18

[a]Mean of 20 measurements.

[b]Mean of 20 measurements with 10 mL min^{-1} Kr or 10 mL min^{-1} Xe.

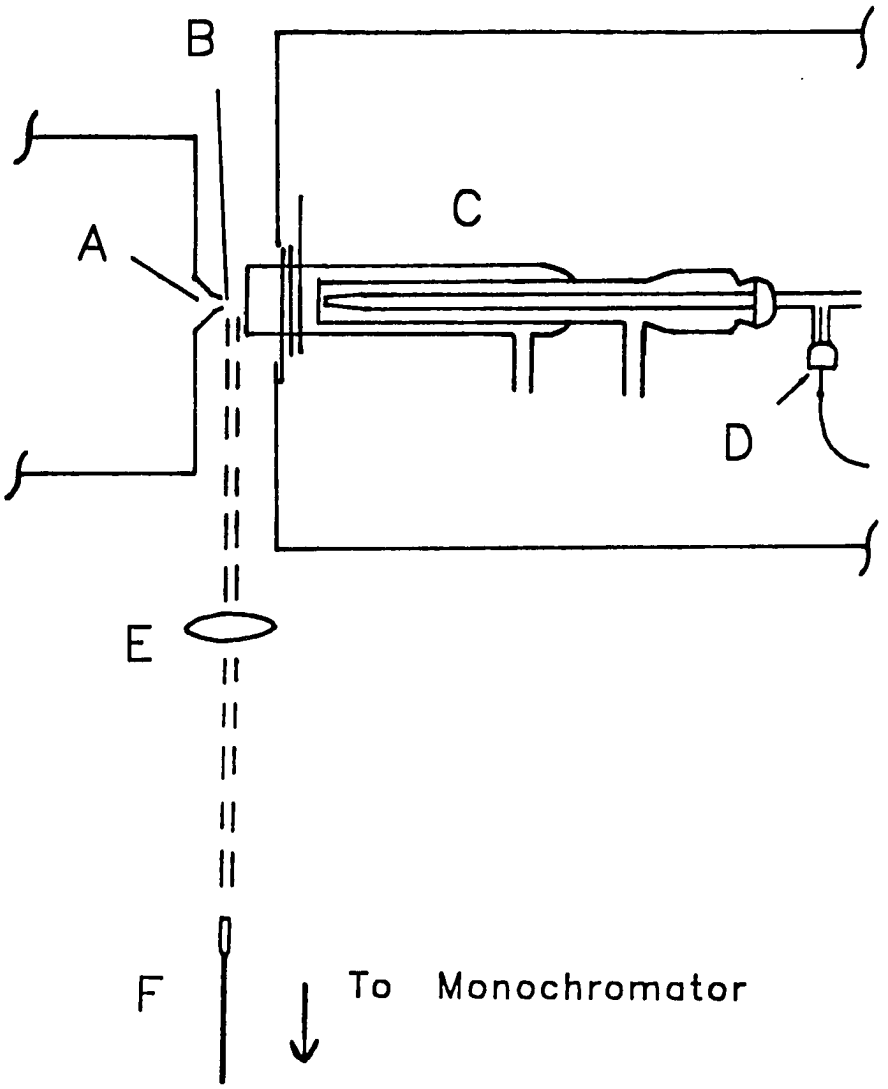

Figure 1. Spatial arrangement of (A) sampler on ICP-MS interface, (B) region viewed by monochromator, (C) ICP torch, (D) glass tee for introduction of Xe or Kr, (E) lens, (F) fiber optic. Distance from sampler to lens is ~24 cm

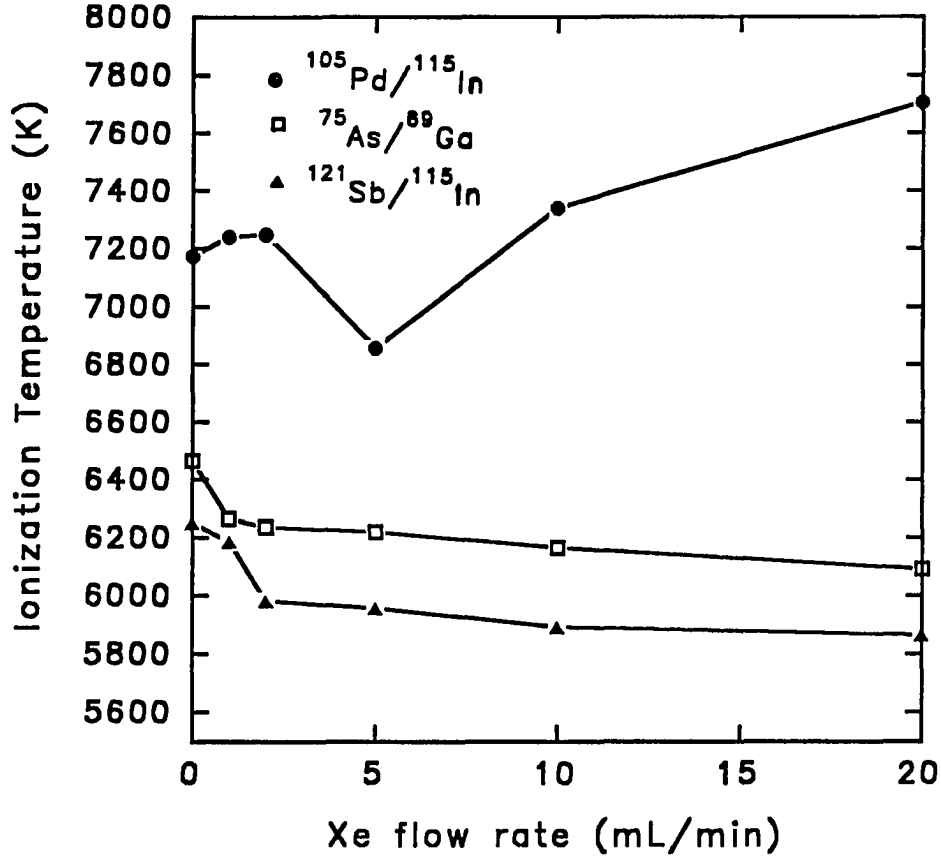

Figure 2. Variation of ionization temperature with increasing Xe flow rate for several thermometric pairs

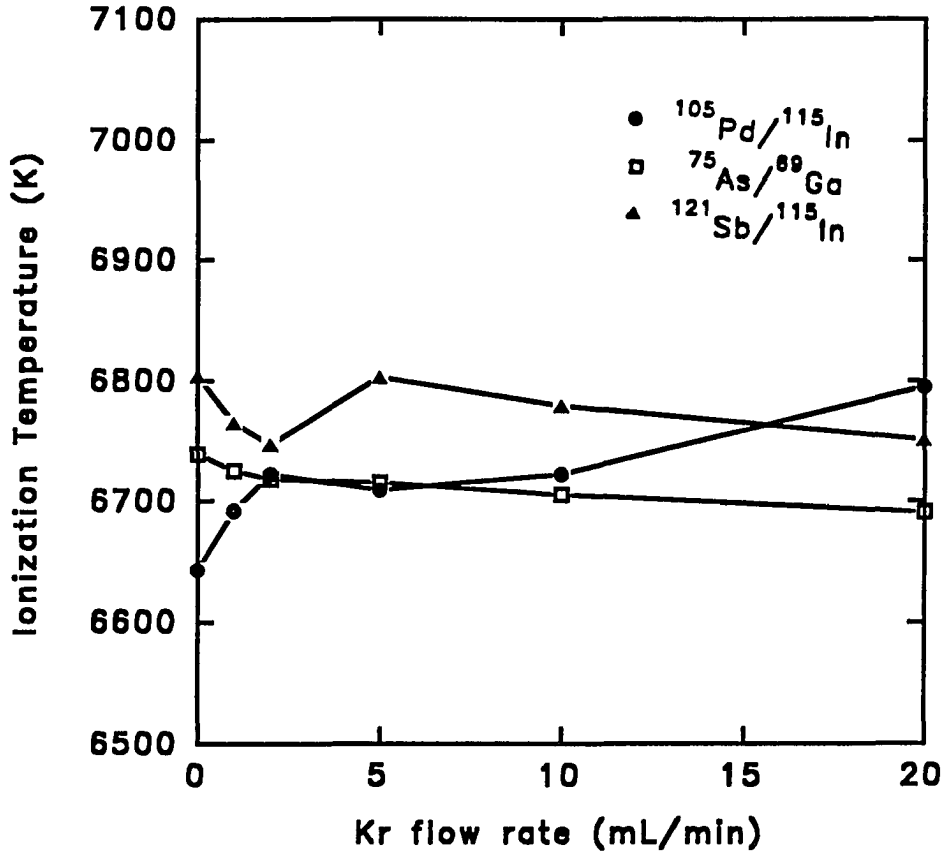

Figure 3. Variation in ionization temperature with increasing Kr flow rate for several thermometric pairs

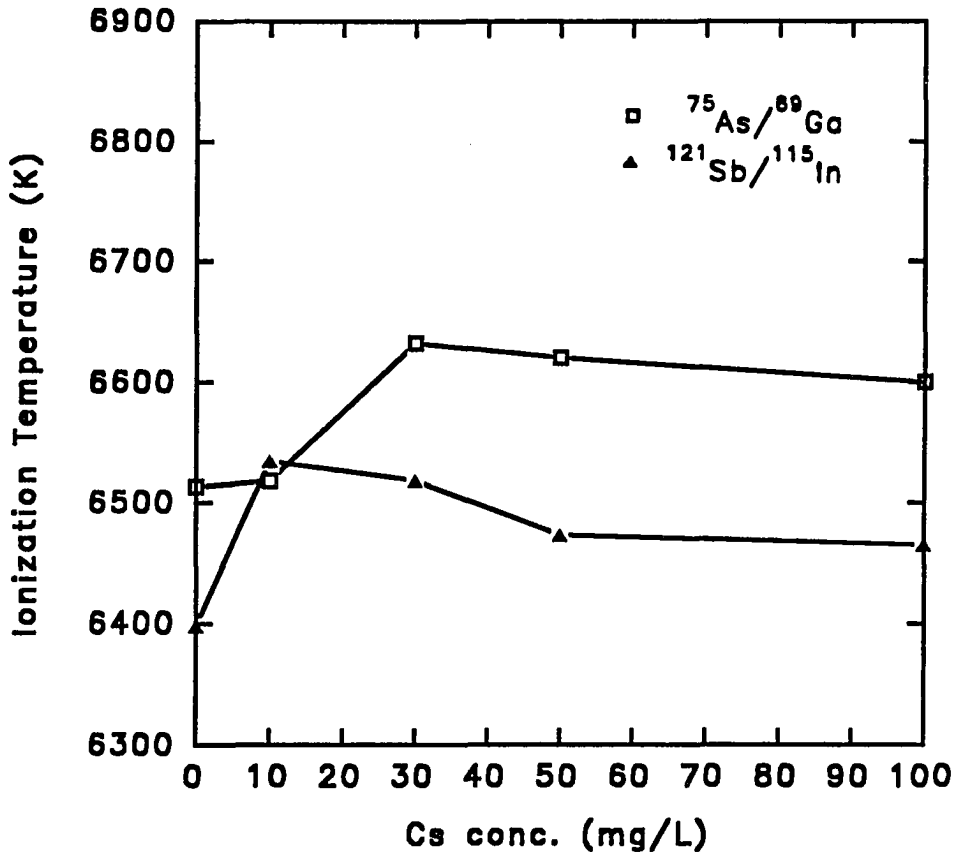

Figure 4. Variation in ionization temperature with increasing Cs concentration for two thermometric pairs

SUMMARY

The primary goal of this work has been the development of new techniques for the determination of hitherto "difficult" elements by ICP-MS. The methods described all involve a new tract in sample preparation and/or sample introduction but no changes in the operating hardware of the ICP or the mass spectrometer. More specifically, these methods reduce sample analysis time and alleviate numerous polyatomic ion interferences. Of course, less analysis time reduces operating costs, but the widened capability of isotope ratio measurements opens the door for new stable isotope tracer studies and further applications of isotope dilution analysis.

Nonetheless, there is much room for improvement and further research in these new techniques. For example, the chlorine method requires 99.9% D_2O, a substance which presently costs approximately fifty cents per milliliter. The expense of preparing a large number of samples in D_2O (~ 5 mL per sample) and having a sufficient volume of D_2O for cleanout of the ultrasonic nebulizer (usually ~ 3 mL) between each sample would be considerable. However, use of the DIN would easily reduce this problem (84). A large sample loop of 20 mL could be installed in a separate flow injection valve ahead of the gas displacement pump. A second flow injection valve ahead of the first could be used for sample loading. Since the DIN operates at a low sample flow rate (~ 120 μL min^{-1}), the reservoir of D_2O would last

almost three hours. In addition, the sample volume need be only 0.1 to 1.0 mL, facilitating concentration of the analyte and enhanced sensitivity. Furthermore, the low dead volume (~ 2 μL) of the transfer line provides rapid sample cleanout (~ 15 s), so any last vestiges of water should be easily removed with consequent lower $^{36}ArH^+$.

Problems with the determination of boron in biological samples point towards sample preparation. There is an elevated background due to the Na_2CO_3 blank, so a more dilute Na_2CO_3 solution should reduce this background as long as sufficient Na_2CO_3 is still available to prevent loss of boron during sample fusion. Since the boron content is at ng g^{-1} levels in samples like human blood plasma, study of boron preconcentration is also desirable. Variables for investigation include ion-exchange resin volume and concentration and volume of HNO_3 for boron elution.

Like D_2O, cost is a major consideration for use of xenon. Depending upon availability, a 100-L tank of xenon currently costs between $1500 and $2000. One possible approach to reduce xenon consumption would be the use of cryogenic desolvation (85). This technique uses a second condenser at -80 ^oC after the first at -10 ^oC. Water loading into the ICP is reduced due to the lowered vapor pressure of water. Therefore, the intensities of polyatomic ions like HN_2^+, NO^+, ArH^+, ClO^+, and ArO^+ should be lower. Consequently, the amount of xenon needed to reduce these ions should be less.

In addition to the water-derived ions listed above, CO_2 impurity in argon and CO_2 from the atmosphere is a troublesome interferent. The ion CO_2^+ interferes with $^{44}Ca^+$, the most abundant minor isotope of calcium. Since CO_2^+ is a high energy ion (I.E. = 13.7 eV), addition of xenon should considerably reduce its intensity. Although the signal from $^{44}Ca^+$ should also be reduced, the combination of the low ionization energy of calcium (6.1 eV) and its abundance in many samples should still yield substantial signal.

Other possible experiments include addition of xenon to the auxiliary and/or outer gas of the ICP and to the make-up gas of the DIN. The effects of xenon on background or analyte ion intensities via the former gas flows is presently unknown. However, since no desolvation of the aerosol is used with the DIN, the intensities of water-derived polyatomic ions may be considerable. Xenon addition could prove helpful in alleviating that problem.

ADDITIONAL LITERATURE CITED

1. Fassel, V. A.; Kniseley, R. N. Anal. Chem. 1974, 46, 1110A, 1155A.
2. Fassel, V. A. Science 1978, 202, 183.
3. Barnes, R. M. Crit. Rev. Anal. Chem. 1978, 7, 203.
4. Gray, A. L. Analyst 1975, 100, 289.
5. Gray, A. L. Anal. Chem. 1975, 47, 600.
6. Houk, R. S.; Fassel, V. A.; Flesch, G. D.; Svec, H. J.; Gray, A. L.; Taylor, C. E. Anal. Chem. 1980, 52, 2283.
7. Pendelbury, D. The Scientist 1988, 2, 20.
8. Houk, R. S. Anal. Chem. 1986, 58, 97A.
9. Houk, R. S.; Thompson, J. J. Mass Spectrom. Revs. 1988, 7, 425.
10. Houk, R. S. In Handbook of Physics and Chemistry of Rare Earths; Gschneidner, K. A., Jr., Eyring, L., Eds.; Elsevier: London, 1990; pp 385-421.
11. Date, A. R.; Gray, A. L. Application of Inductively Coupled Plasma Mass Spectrometry; Blackie and Sons Ltd.: London, 1988.
12. Miller, P. E.; Denton, M. B. J. Chem. Ed. 1986, 63, 617.
13. Kurz, E. A. Am. Lab. March 1979, 11, 67.
14. Mochizuki, T.; Sakashita, A.; Iwata, H.; Ishibashi, Y.; Gunji, N. Anal. Sci. 1989, 5, 311.
15. Ebdon, L.; Foulkes, M. E.; Parry, H. G. M.; Tye, C. T. J. Anal. At. Spectrom. 1988, 3, 753.

16. Gregoire, D. C. J. Anal. At. Spectrom. 1988, 3, 309.

17. Park, C. J.; Hall, G. E. M. J. Anal. At. Spectrom. 1988, 3, 355.

18. Dickin, A. P.; McNutt, R. H.; McAndrew, J. I. J. Anal. At. Spectrom. 1988, 3, 337.

19. McLaren, J. W.; Beauchemin, D.; Berman, S. S. Spectrochim. Acta, Part B 1988, 43B, 413.

20. Hirata, T.; Shimizu, H.; Akagi, T.; Sawatari, H.; Masuda, A. Anal. Sci. 1988, 4, 637.

21. Kantipuly, C. J.; Westlund, A. D. Talanta 1988, 35, 1.

22. Jarvis, K. E. Chem. Geol. 1988, 68, 31.

23. Hall, G. E. M.; Bonham-Carter, G. F. J. Geochem. Explor. 1988, 30, 255.

24. Date, A. R.; Cheung, Y. Y.; Stuart, M. E.; Jin, X. J. Anal. At. Spectrom. 1988, 3, 653.

25. Date, A. R.; Cheung, Y. Y. Analyst 1987, 112, 1531.

26. Parry, H. G. M.; Ebdon, L. Anal. Proc. 1988, 25, 69.

27. Kantipuly, C. J.; Longerich, H. P.; Strong, D. F. Chem. Geol. 1988, 69, 171.

28. Douglas, D. J.; French, J. B. J. Anal. At. Spectrom. 1988, 3, 743.

29. Beauchemin, D.; Berman, S. S. Anal. Chem. 1989, 61, 1857.

30. Beauchemin, D.; McLaren, J. W.; Mykytiuk, A. P.; Berman, S. S. J. Anal. At. Spectrom. 1988, 3, 305.

31. Taylor, H. E.; Garbarino, J. R. J. Res. Natl. Bur. Stand. 1988, 93, 433.

32. Garbarino, J. R.; Taylor, H. E.; Batie, W. C. Anal. Chem. 1989, 61, 793.

33. Henshaw, J. M.; Heithmar, E. M.; Hinners, T. A. Anal. Chem. 1989, 61, 335.

34. Hall, G. E. M.; Jefferson, C. W.; Michel, F. A. J. Geochem. Explor. 1988, 30, 63.

35. Date, A. R.; Stuart, M. E. J. Anal. At. Spectrom. 1988, 3, 659.

36. Bakowska, E.; Falkner, K. K.; Barnes, R. M.; Edmond, J. M. Appl. Spectrosc. 1989, 43, 1283.

37. Dunn, C. E.; Hall, G. E. M.; Hoffman, E. J. Geochem. Explor. 1989, 32, 211.

38. Brzezinska-Paudyn, A.; Van Loon, J. C. Fresenius' Z. Anal. Chem. 1988, 331, 707.

39. Northington, D. J. Am. Ind. Hyg. Assoc. J. 1987, 48, 977.

40. Beauchemin, D.; McLaren, J. W.; Berman, S. S. J. Anal. At. Spectrom. 1988, 3, 775.

41. Newman, R. A.; Osborn, S.; Siddik, Z. H. Clin. Chim. Acta 1989, 179, 191.

42. Heitkemper, D.; Creed, J.; Caruso, J.; Fricke, F. L. J. Anal. At. Spectrom. 1989, 4, 279.

43. Shibata, Y.; Morita, M. Anal. Sci. 1989, 5, 107.

44. Bushee, D. S. Analyst 1988, 113, 1167.

45. Beauchemin, D.; McLaren, J. W.; Willie, S. N.; Berman, S. S. Anal. Chem. 1988, 60, 687.

46. Berman, S. S.; Siu, K. W. M.; Maxwell, P. S.; Beauchemin, D.; Clancy, V. P. Fresenius' Z. Anal. Chem. 1989, 333, 641.

47. Beauchemin, D.; Siu, K. W. M.; Berman, S. S. Anal. Chem. 1988, 60, 2587.

48. Beauchemin, D.; Bednas, M. E.; Berman, S. S.; McLaren, J. W.; Siu, K. W. M.; Sturgeon, R. E. Anal. Chem. 1988, 60, 2209.

49. Shibata, Y.; Morita, M. Anal. Chem. 1989, 61, 2116.

50. Ridout, P. S.; Jones, H. R.; Williams, J. G. Analyst 1988, 113, 1383.

51. Schuette, S.; Versault, D.; Ting, B. T. G.; Janghorbani, M. Analyst 1988, 113, 325.

52. Ting, B. T. G.; Mooers, C. S.; Janghorbani, M. Analyst, 1989, 114, 667.

53. Woodhead, J. C.; Drulis, J. M.; Rogers, R. R.; Ziegler, E. E.; Stumbo, P. H.; Janghorbani, M.; Ting, B. T. G.; Fomon, S. J. Pediatr. Res. 1988, 23, 495.

54. Fomon, S. J.; Janghorbani, M.; Ting, B. T. G.; Ziegler, E. E.; Rogers, R. R.; Nelson, S. E.; Ostedgaard, L. S.; Edwards, B. B. Pediatr. Res. 1988, 24, 20.

55. Janghorbani, M.; Davis, T. A.; Ting, B. T. G. Analyst 1988, 113, 405.

56. Sun, X. F.; Ting, B. T. G.; Janghorbani, M. Anal. Biochem. 1987, 167, 304.

57. Whittaker, P. G.; Lind, T.; Williams, J. G.; Gray, A. L. Analyst 1989, 114, 675.

58. Campbell, M. J.; Delves, H. T. J. Anal. At. Spectrom. 1989, 4, 235.

59. Delves, H. T.; Campbell, M. J. J. Anal. At. Spectrom. 1988, 3, 343.

60. Templeton, D. M.; Paudyn, A.; Baines, A. D. Biol. Trace Elem. Res. 1989, 22, 17.

61. Gladney, E. S.; Moss, W. D.; Guatier, M. A.; Bell, M. G. Health Phys. 1989, 57, 171.

62. Crews, H. M.; Dean, J. R.; Ebdon, L.; Massey, R. C. Analyst 1989, 114, 895.

63. Lyon, T. D. B.; Fell, G. S.; Hutton, R. C.; Eaton, A. N. J. Anal. At. Spectrom. 1988, 3, 265.

64. Vanhoe, H.; Vandecasteele, C.; Versieck, J.; Dams, R. Anal. Chem. 1989, 61, 1851.

65. Yoshinaga, J.; Nakazawa, M.; Suzuki, T.; Morita, M. Anal. Sci. 1989, 5, 355.

66. Crews, H. M.; Massey, R.; McWeeny, D. J.; Dean, J. R. J. Res. Natl. Bur. Stand. 1988, 93, 349.

67. Thompson, J. J.; Houk, R. S. Anal. Chem. 1988, 58, 2541.

68. VanLoon, J. C.; Alcock, L. R.; Pinchin, W. H.; French, J. B. Spectrosc. Lett. 1986, 19, 1125.

69. Chong, N. S.; Houk, R. S. Appl. Spectrosc. 1987, 41, 66.

70. McLeod, C. W. J. Anal. At. Spectrosc. 1987, 2, 549.

71. Dean, J. R.; Munro, S.; Ebdon, L.; Crews, H. M.; Massey, R. C. J. Anal. At. Spectrosc. 1987, 2, 607.

72. Meinhard, J. E. In Applications of Plasma Emission Spectrochemistry; Barnes, R. M., Ed.; Heyden: Philadelphia, 1979; pp 1-14.

73. Hulmston, P. Analyst 1983, 108, 166.

74. Ramsey, M. H.; Thompson, M.; Coles, B. J. Anal. Chem. 1983, 55, 2626.

75. Baginski, B. R.; Meinhard, J. E. Appl. Spectrosc. 1984, 38, 568.

76. Zhuang, H. Z.; Barnes, R. M. Spectrochim. Acta, Part B 1985, 40B, 11.

77. Veillon, C.; Margoshes, M. Spectrochim. Acta, Part B 1968, 23B, 553.

78. Boumans, P. W. J. M.; DeBoer, F. J. Spectrochim. Acta, Part B 1976, 31B, 355.

79. Olson, K. W.; Haas, W. J., Jr.; Fassel, V. A. Anal. Chem. 1977, 49, 632.

80. Goulden, P. D.; Anthony, D. H. J. Anal. Chem. 1984, 56, 2327.

81. Fassel, V. A.; Bear, B. R. Spectrochim. Acta, Part B 1986, 41B, 1089.

82. Vaughn, M. A.; Horlick, G. Appl. Spectrosc. 1986, 4, 434.

83. Tan, S. H.; Horlick, G. Appl. Spectrosc. 1986, 4, 445.

84. Wiederin, D. R.; Smith, F. G.; Houk, R. S. Anal. Chem. 1991, 63, 219.

85. Wiederin, D. R.; Houk, R. S.; Winge, R. K.; D'Silva, A. P. Anal. Chem. 1990, 62, 1155.

ACKNOWLEDGMENT

First and foremost I would like to thank my parents Harry and Carmen Smith for all of their support during the years of my education. The journey from Gospel to Iowa State has been long, difficult, and often dangerous, and they alone understand this. I would also like to thank my Uncle Fred for helping me financially several times while in college. As Jack Thiede says, he can be rather gruff, but when you're in a jam, he'll help you out.

I am also grateful to my major professor, Dr. Sam Houk. He always took the time to talk to me about my research, and he taught me a great deal about scientific writing. I also enjoyed all of our discussions about sports and history. I would also like to thank Sam's wife Linda for saving me from a long night at the bus station in Des Moines during my first visit to Iowa State.

Since I have been in the Houk group since 1985, I consider myself the last of the "old gang". In fact, I go back all the way to the great J. J. Thompson. There are many former group members I would like to thank for their help: S.-J. Jiang, John Rowan, Jon Schoer, Jeff Crain, and H. B. Lim. I would particularly like to thank Dan Wiederin and his wife Michelle for all their help and kindness, especially during holidays when I had no place to go. I wish Sam Shum, Luis Alves, Ke Hu, Hongsen Niu, Rocky Warren, Scott Clemons,

Shen Luan, Xiaoshan Chen, and Steve Gilles (our adopted group member) all the best. I always enjoyed your company.

There are many other people outside the Houk group I wish to thank, especially Dr. Robert Serfass and Claire Egan for their help with the boron project. I am grateful to Art D'Silva for all of his sage advice and to his son Colin for showing me the variety of life in Cleveland. I also wish to thank Royce Winge for his help with the emission spectrometer. Finally, I wish to thank Jim Goll, Dan and Julie Bougie, and John Nedderson for their friendship and all the rides back to Wisconsin, our home.

I did not know what to expect when I entered graduate school six years ago, and some things I was not prepared for: getting punched on Cy-Ride, the frustrations of research, ridicule and humiliation, a broken heart, and the necessity of spending lots of money to improve my personal appearance. I apologize to anyone I offended with my often sour and pessimistic disposition. But in any event, I would like people to know that Fred is just a regular guy from Milwaukee who does the best he can.

This work was performed at the Ames Laboratory under contract no. W-7405-ENG-82 with the U. S. Department of Energy. The United States government has assigned DOE report no. IS-T-1552 to this dissertation.